The Pennsylvania State University

The Graduate School

Department of Biology

A GENETIC SCREEN FOR SECOND CHROMOSOME MODIFIERS OF A TEMPERATURE-SENSITIVE PRESYNAPTIC CALCIUM CHANNEL MUTANT OF *DROSOPHILA*

A Thesis in

Biology

by

Shaona Acharjee

Submitted in Partial Fulfillment
of the Requirements
for the Degree of

Doctor of Philosophy

May 2008

The thesis of Shaona Acharjee was reviewed and approved* by the following:

Richard Ordway, Associate Professor of Biology
Thesis Advisor
Chair of Committee

Kyuang Han
Associate Professor of Biology

Zhi-Chun Lai
Associate Professor of Biology, Biochemistry and Molecular Biology

Wendy Hanna-Rose
Assistant Professor of Biochemistry and Molecular Biology

Douglas Cavener
Profssor of Biology
Head of the Department of Biology

*Signatures are on file in the Graduate School

ABSTRACT

Synaptic release of chemical neurotransmitters is triggered by calcium influx through presynaptic voltage-gated calcium channels. In *Drosophila*, the molecular basis of presynaptic calcium channel function has been defined through analysis of cac^{TS2}, a temperature-sensitive (TS) paralytic mutant of the calcium channel α_1 subunit gene, *cacophony*. The cac^{TS2} mutant has also served as a starting point for further genetic analysis. To broaden our understanding of the functions and interactions of *cac*-encoded calcium channels, we conducted a screen for second chromosome genetic modifiers of the cac^{TS2} paralytic phenotype. Two mutations have been recovered as enhancers of cac^{TS2}. Electrophysiological analysis indicates these mutations affect synaptic transmission. Both the mutations are alleles of the same gene. Meiotic and deficiency mapping has placed both the mutations in the right arm of the second chromosome within the cytological region 54D4-54D5. Molecular characterization is expected to identify the mutation locus and further define the *in vivo* roles of the gene products in this process.

The work presented in this thesis outlines the background of the project in the first chapter. Molecular mechanisms of signal transmission

at chemical synapses, the role of voltage gated calcium channels at the presynaptic terminals and the utility of TS mutants in studying the synaptic transmission have been discussed. The genetic screen for second chromosome modifiers of cac^{TS2} TS paralytic phenotype followed by phenotypic and genotypic characterization of the modifiers obtained from the screen has been described in the second and third chapter. These results have been discussed in referencd to the current understanding of the synaptic transmission. The mutants recovered in this screen are either novel TS alleles of previously characterized genes or may identify new members of the molecular machinery governing the synaptic transmission.

TABLE OF CONTENTS

LIST OF FIGURES vii

LIST OF TABLES xi

LIST OF ABBREVIATIONS xii

ACKNOWLEDGEMENTS xiii

Chapter 1 INTRODUCTION 1

1.1 Overview of Synaptic Transmission 1

1.2 Active Zones: Zone of Vesicle Fusion 2
1.3.1 Fusion of Synaptic Vesicles 4
1.3.2 Vesicle Recycling: Classical Endocytosis and Kiss and Run 5
1.3.3 Synaptic Vesicle Pools 6
1.3.4 Core Proteins in Synaptic Vesicle Fusion 8
1.4 Presynaptic Voltage Gated Calcium Channels 10
1.4.1 α_1 Subunit of Voltage Gated Calcium Channels 13
1.4.2.1 β Subunit 14
1.4.2.2 $\alpha_2\delta$ Subunit 15
1.4.3 Calcium Channel Regulatory Proteins 15
1.6 Temperature Sensitive (TS) Mutants in *Drosophila* 18
1.7 Discovery and Characterization of a TS Paralytic Mutant of a Presynaptic Calcium Channel (*cac*^{TS2}) 19
1.8 Modifier Screen for *cac*^{TS2} Paralytic Phenotype 21
1.9 Genetic Screen for Second Chromosome Modifiers of *cac*^{TS2} Paralytic Phenotype 22

Chapter 2 GENETIC SCREEN TO IDENTIFY SECOND CHROMOSOME MODIFIERS OF cac^{TS2} MUTANTS IN *DROSOPHILA* 23

2.1 Overview 23
Drosophila Stocks 24
Data analysis 26
2.3.1 A Screen for Second Chromosome genetic modifiers of *cac*^{TS2} 26
2.3.2 TS Paralytic Behavior of the Enhancers 29
2.3.2.1 Recovery of Two Enhancers, e(cac)2902 and e(cac)3063, that have altered cac^{TS2} TS paralytic and synaptic phenotype 29

2.3.3 Isolation of *e(cac)2902* and *e(cac)3063* from the cac^{TS2} Genetic Background 30
2.3.3.1 TS Paralytic Behavior of e(cac)2902 and e(cac)3063 in Wild Type Background 31
2.3.3.2 e(cac)2902 and e(cac)3063 are Alleles of the Same Gene 32
2.3.3.3 Synaptic Physiology of e(cac)2902 and e(cac)3063 in a cac^{TS2} or Wild-Type Genetic Background 33

Chapter 3 36

GENETIC MAPPING OF THE ENHANCERS *e(cac)2902* AND *e(cac)3063* 36

3.1 Overview 36
3.2 Materials and Methods 36
3.3 Results 39
3.3.1 Complementation Test with the Deficiency Chromosomes for Genes known to be involved in Synaptic Regulation 39
3.3.2 Meiotic Mapping 40
3.3.3 Replace with Subject Heading 41
3.3.3 Deficiency Mapping 42
3.4 Genes Present in the Region 54D1-54D4 44

Chapter 4 Discussion 47

Chapter 5 Appendices 52

Appendix A: Analysis of Synaptic Physiology in Transgenic Flies Expressing Tetanus Toxin 52

A.1 Introduction 52

A.2 Material and Methods 54

A.3 Result 55

A.4 Discussion 56

Appendix B: 57

Generation of transgenic fly lines carrying FLAG or tdTomato tagged calcium channel Beta subunit 57

B.1 Introduction 57
B.2 Generation of DNA Construct carrying Calcium Channel β Subunit fused with FLAG or tdTomato 58
B.2.1 DNA construct of calcium channel β subunit – tdTomato transgene 58
B.2.2 DNA construct of calcium channel β subunit – FLAG transgene 60

B.4 Verification of the Transgene Expression 63

B.4.1 β- FLAG 63
B.4.2 Beta tdTomato 64

Bibliography 66

LIST OF FIGURES

Figure 1.1 Schematic Diagram of a Chemical Synapse. Synapse consists of a presynaptic terminal plasma membrane and a postsynaptic membrane which are separated by a narrow cleft. The presynaptic terminal contains synaptic vesicles packed with neurotransmitters (represented as blue circle). An action potential traveling down the axon causes the plasma membrane to depolarize. The voltage gated calcium channels (VGCC) open in response to the depolarization and allow calcium to enter the cell. Calcium, in turn, triggers the fusion of synaptic vesicles with the plasma membrane. Upon fusion, the vesicles release neurotransmitters that bind to the postsynaptic receptors and trigger generation of electrical potentials in the postsynaptic membrane. 2

Figure 1.2: Electron Micrograph of *Drosophila* Larva Neuromuscular Junction. (a) The presynaptic terminal of a motor neuron is surrounded by muscle fibers on all sides. Electron dense structures called T-Bars. are observed at the junction of the nerve and the muscles. (b) The T-Bars represent the active zone, the region where the vesicles cluster, tether and fuse at the presynaptic terminal. The spherical vesicles can be observed around the T-Bar. Figure modified from *Atwood, 2006* [1]. 3

Figure 1.3: Steps in Synaptic Vesicle Fusion. Vesicle fusion is a multistage process that includes docking, priming, fusion and recycling. 4

Figure 1.5: Three Vesicle Pools. The vesicle can be functionally grouped into three groups: readily releasable pool (RRP), recycling pool and reserve pool. The RRP is available for immediate use, the recycling pool is used during normal physiological stimulation and the reserve pool forms the depot of vesicles. These pools, however, can be segregated visually..... 7

Figure 1.7: Calcium Channels as Key Signal Transducers at the Synapse. Ca channels can be modeled as key signal transducers analogous to other membrane associated signaling systems, as for example, G-protein coupled receptors. In this pathway, a stimulus causes to generate action potential, which in turn, causes membrane depolarization. Depolraization leads to the opening of voltage gated calcium channel. The Ca influx increases

intracellular calcium concentration. Thus, Ca acts as a diffusible second messenger and triggers the cellular event, vesicle fusion (Adopted from Zamponi, 2005 [31]. 11

Figure 1.8: Voltage Gated Calcium Channel (VGCC). The VGCCs are heteromultimers composed of four or five subunits: the primary α_1 subunit and the auxiliary β, $\alpha_2\delta$ and possibly a γ subunit. The α_1 subunit is composed of four domains I-IV. The AID or the alpha1 interacting domain is the site of interaction between α_1 and β subunit. Figure modified from Petegam, 2006 [34]..... 12

Figure 1.9: Topology of α_1 Subunit of Calcium Channel. Roman numerals refer to the four repeating domains, each consisting of six transmembrane segments (S1-S6). The charged S4 segment is thought to act as a voltage sensor. Both the N and C termini are intracellular. The calcium binding domain (EF hand) and the calcium calmodulin binding domain (IQ) are present within the C-terminal cytoplasmic domain. 14

Figure 1.10: The *cac^{TS2}* mutation. Alignment of CAC with related calcium-channel a1 subunit polypeptide sequences is shown. Amino acid identities with CAC are shaded. Boxed sequences correspond to the EF hand and a portion of the IVS6 transmembrane segment. The cacTS2 mutation, P1385S, maps to an invariant proline residue adjacent to the EF hand. The aligned sequences correspond to CAC, rat brain α_1A and α_1B and C.elegans UNC-2, respectively [58]. 20

Figure 1.11: Synaptic Physiology of cacTS2 mutant. Representative Excitatory Postsynaptic Current (EPSC) recordings from dorsal longitudinal flight muscle (DLM) neuromuscular synapses of wild type (WT) and *cac^{TS2}* at 20°C and 36°C. *cac^{TS2}* exhibits a wild-type EPSC amplitude at 20°C. At the restrictive temperature of 36°C, the EPSC amplitude is significantly reduced relative to WT. This change is reversible; the EPSC amplitude recovers when the temperature is brought back to 20°C. The extent of current reduction was dependent on the temperature, at 38°C; the EPSC amplitude was further reduced in comparison to 36°C. Stimulation artifacts were removed for clarity. All recordings were performed on flies reared at 20°C. *Modified from Kawasaki, 2000[46]*. 21

Figure 2.1: A F_3 Genetic Screen for modifiers of *cac^{TS2}* 27

Figure 2.2: Overview of the Genetic Screen. Percentages of F_3 progeny produced in the F_3 screen were consistent over time. 5400 F_1 crosses were divided in groups of one hundred and the value for each group was plotted. Homozygous viable flies were screened for an enhanced or suppressed *cac^{TS2}* behavior phenotype at 36°C..... 28

Figure 2.4: TS Paralytic Behavior of *e(cac)2902* and *e(cac)3063*. Two double mutants selected for further study, *w* cac^{TS2}*; e(cac)2902 and w* cac^{TS2}*; e(cac)3063* exhibit rapid paralysis at 36°C, whereas cac^{TS2} alone does not paralyze at this temperature. cac^{TS2} behavioral tests were truncated after 20 min. Flies heterozygous for the enhancer mutation, cac^{TS2}; e(cac)2902/+ and w cac^{TS2}; e(cac)3063/+, behaved like cacTS2 showing that both mutations are recessive. Asterisks mark values significantly different from control values. 30

Figure 2.5: Scheme for Isolating the Enhancer Mutations from the *cacTS2* background. 31

Figure 2.6: **TS Paralytic Behavior of *e(cac)2902* and *e(cac)3063*.** *w; e(cac)2902 and w; e(cac)3063* exhibit rapid paralysis at 38°C. WT behavioral tests were truncated after 20 min. Asterisks marks indicate significant difference. 32

Figure 2.7: Synaptic Physiology of a Second Chromosome Enhancer of cacTS2. (A) Representative Excitatory Postsynaptic Current (EPSC) recordings from dorsal longitudinal flight muscle (DLM) neuromuscular synapses of wild type (WT), *cacTS2*, and the *w cacTS2; e(cac)2902* double mutant and *w; e(cac)2902* at 20°C and 36°C. *w cacTS2; e(cac)2902* and *w; e(cac)2902* exhibit a wild-type EPSC amplitude at 20°C. At the restrictive temperature of 36°C, the EPSC amplitude of *w cacTS2; e(cac)2902* is significantly reduced relative to both WT and cacTS2 alone. *w; e(cac)2902* amplitude is signicantly reduced compared to WT. Stimulation artifacts were removed for clarity. The 36°C recordings were obtained after 7 min at 36°C. All recordings were performed on flies reared at 20°C. (B) Mean EPSC amplitudes. SEM are represented by the error bars. Asterisks indicate the differences are statistically significant. 33

Figure 3.1: Recombinants arise from meioses in which nonsister chromatids cross over between the genes under study. *A* and *B* are two dominant mutations of *a* and *b* respectively. The black spot designate the mutation whose position is to be estimated relative to the position of *A* and *B*. *Figure modified from* Introduction to Genetic Analysis [63] 38

Figure 3.2: Complementation Test with deficiency chromosomes. The deficiency chromosomes (green and blue lines) are produced from chromosomal aberration or rearrangement in which a piece of the chromosome is excised and the remaining large pieces are reattached. If the mutation locus (marked with asterisk) fell within the region of deletion, deficiency chromosome would not complement the mutation, leading to TS paralytic behavior. Conversely, complementation would indicate that the mutation is not present in the region of deletion. 39

Figure 3.3: Meiotic Mapping. (A) The position of the visible markers in the second chromosome that were used for mapping. (B) The genetic scheme to produce recombinant flies.(C) Recombination mapping placed the mutation within 54A-57B cytological units (the region marked in red).....41

Figure 3.4: Deficiency Mapping for *e(cac)2902* and *e(cac)3063*. (A) Recombination mapping placed the mutation within cytological region 54A-57B. For narrowing down the region of mutation loci, deficiency chromosomes were used in which parts of the chromosome within the region 54A-57B was deleted. (B) The deletions in the deficiency chromosomes are shown as black or blue lines. The deficiencies represented by black lines complemented the mutations. The blue lines correspond to the deficiencies that failed to complement the enhancer mutations. The deficiency mapping suggested that the enhancer locus fell within a region of ~150kbp between 54D1-54E7 (C) Smaller deficiencies, indicated by blue, black or orange lines, were used to further reducing the region containing the enhancer locus. The orange lines correspond to the deficiencies that failed to complement the enhancer mutations and placed the mutation within a region of ~20kbp between 54D4-54D5.....43

Figure 3.5: Candidate Genes present in the region containing the mutation loci for *e(cac)2902* and *e(cac)3063*. The mutation was mapped to the cytological map units 54D4-D5. This corresponded to the sequence co-ordinate 13553k-13575k. The spans of the seven genes that encompass this region are shown in this figure. The genes' coding sequences (CDS) are also shown.....44

Figure A.1: Structure of tetanus toxin. The light chain (L_C) and a heavy chain (H_C) of tetanus toxin are formed by the proteolytic cleavage of a pre-protein. A disulphide linkage joins the L_C and the H_C.....53

Figure A.2: Synaptic Physiology of OK6-Gla4; UAS-TNT (A) Representative Excitatory Postsynaptic Current (EPSC) recordings from neuromuscular synapses of muscle 6 of the abdominal segments A2 or A3 of wild type (WT) and OK6-Gla4; UAS-TNT at 20°C.. Stimulation artifacts were removed for clarity. OK6-Gla4; UAS-TNT flies were reared at 25°C (B) Mean EPSC amplitudes. SEM are represented by the error bars.....55

Figure B.2: Expression level of β-FLAG in the transgenic lines was detected by Western Blot. An anti-FLAG antibody was used to detect β FLAG (48.6 kDa). Only one line is shown in this figure as an example. The antibody also detected a nonspecific band in the transgenic line with molecular weight ~65KDa. Tubulin was used as a loading control.....63

Figure B.3: Live imaging of β-tdTomato at larval neuromuscular synapses. Images were acquired with a Nikon (Tokyo, Japan) Eclipse E600FN microscope equipped with a Fluor 60X 1.0 numerical aperture water-immersion objective (Nikon) and the following filter set: excitation filter, 555/25; dichroic mirror, 565DCLP; and emission filter, D620/60 (Chroma, Brattleboro, VT). Image capture was carried out using a CCD camera (ORCA-ER; Hamamatsu Photonics, Hamamatsu, Japan) controlled by MetaVue software (Universal Imaging, Ypsilanti, MI)..... 64

LIST OF TABLES

Table 2.1: EPSC Amplitudes Recorded from DLM of TS paralytic Mutants at Permissive and Restrictive Temperature..... 34

Table 3.1: Complementation Test with Deficiency Chromosome for Known Genes..... 40

Table 4.1: *Drosophila* TS Paralytic Mutants..... 49

LIST OF ABBREVIATIONS

AID	alpha-1 interacting domain
AP	Action Potential
BRP	Bruchpilot Protein
Ca^{2+}	Calcium
CaBP	Calcium Binding Protein
CaM	Calmodulin
cAMP	cyclic Adenosine Mono Phosphate
CDF	Calcium Dependent Facilitation
CDI	Calcium Dependent Inactivation
CyO	Curly of Ostar
Df	Deficiency
DLM	Dorsal Longitudinal Flight Muscles
dNSF1	*Drosophila N*-ethylmaleimide-Sensitive Fusion Protein
EMS	Ethyl Methane Sulphonate
EPSC	Excitatory Postsynaptic Potential
FRT	Flipase Recognition Target
GFP	Green fluorescent poritein
Hc	Heavy chain
Lc	Laight chain
NSF	*N*-ethylmaleimide-Sensitive Fusion Protein
RF	Recombination Frequency
Rim1	Rab3 interacting molecule
RRP	Readily Releasable Pool
Sco	Scutoid
SM	Sec-1/Munc-18
SNAP-25	Synaptosome Associated Protein of 25 kD
SNARE	SNAP Receptor
Sp	Sternopleural
SV	Synaptic Vesicles
TeTx or TNT	Tetanus Toxin
TS	Temperature Sensitive
t-SNARE	Target-SNARE
UAS	Upstram Activator Sequence
VGCC	Voltage Gated Calcium Channel
v-SNARE	Vesicle-SNARE
WT	Wild-Type

ACKNOWLEDGEMENTS

I want to express my gratitude to my Ph.D. mentor, Dr. Richard Ordway, who was a great source of motivation and inspiration. Without him, it would not have been possible to complete my PhD training.

I am grateful to Dr. Fumiko Kawasaki, the project leader for the modifier screen of cac^{TS2} mutants. She guided my study and had a momentous role in my training.

This project would not have been possible without Andre Lutas, Todor Khristov, James Blairle and all other undergraduate students who helped me in the large-scale genetic screen. Andrew, a very talented undergraduate student, worked in this project from the beginning and deserves special appreciation.

Dr. Beiyan Zou, Lisa Posey, Wenhua Yu and Huaru Yan were my colleagues in the lab. We spent a lot of time together in the lab and learnt various research techniques from them. I shall always cherish the memories of our times spent together. I could not have wished for more - thank you my friends.

I want to thank the Department of Biology for giving me the scope to carry out my Ph.D. program. The department has been supportive in this process. I am particularly

thankful to Dr. Chuck Fisher and Ms. Kathryn McClintock for your role in supporting my career development.

This acknowledgement will not be complete without the mention of my friends, Anamika, Arin, Avantika, Benny, Julie, Laura, Malay, Shubhadeep and many others who stood by me in good and bad times.

Finally, I want to thank my parents whose lifelong sacrifice was directed towards my well being. I shall always be indebted to them.

Chapter 1

INTRODUCTION

1.1 Overview of Synaptic Transmission

Transmission of electrochemical signals at the synapses is the principal mode of communication between the neurons. Electrical impulses are generated at the origin of the axon in the form of an action potential (AP). The AP travels down the axon and depolarizes the presynaptic membrane. In response to depolarization, voltage gated calcium channels (VGCCs) present in the presynaptic membrane undergo conformational change and allow calcium to enter the cell. Calcium influx triggers the fusion of synaptic vesicles (SVs) present in the presynaptic terminals with the plasma membrane. Consequently, the neurotransmitters are released and, in this way, an electrical signal is converted to a chemical one. The neurotransmitters released into the synaptic cleft bind to postsynaptic receptors and induce a change in the postsynaptic membrane potential (Figure 1.1).

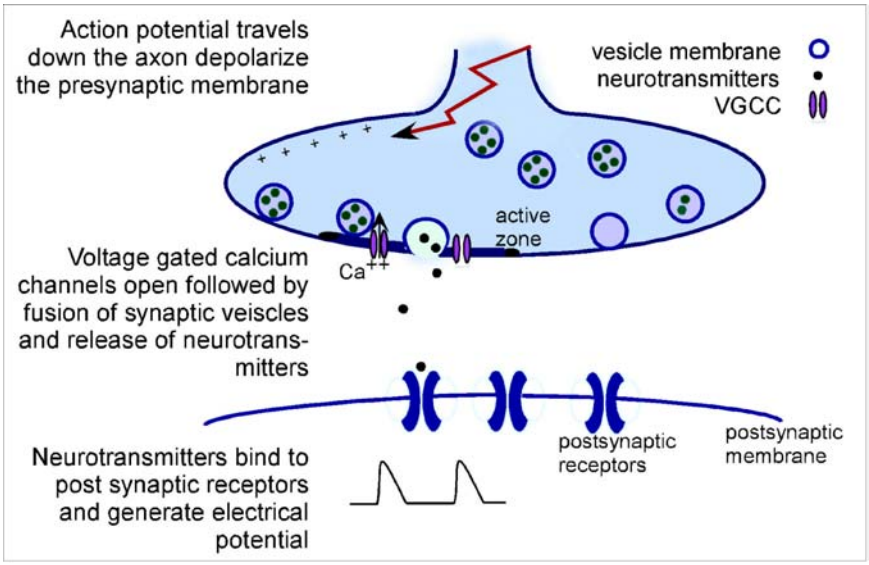

Figure 1.1 Schematic Diagram of a Chemical Synapse. Synapse consists of a presynaptic terminal plasma membrane and a postsynaptic membrane which are separated by a narrow cleft. The presynaptic terminal contains synaptic vesicles packed with neurotransmitters (represented as blue circle). An action potential traveling down the axon causes the plasma membrane to depolarize. The voltage gated calcium channels (VGCC) open in response to the depolarization and allow calcium to enter the cell. Calcium, in turn, triggers the fusion of synaptic vesicles with the plasma membrane. Upon fusion, the vesicles release neurotransmitters that bind to the postsynaptic receptors and trigger generation of electrical potentials in the postsynaptic membrane.

1.2 Active Zones: Zone of Vesicle Fusion

Upon Ca^{2+} entry, the synaptic vesicles fuse at a specialized region in the presynaptic plasma membrane, called the **active zone**. Calcium channels are clustered in the active zone. When viewed under an electron microscope, active zones appear as electron dense structures of 200-300 nm in length [1]. The cytomatrix forming the active zone is arranged in a variety of ways in different species. For example, active zones in *Drosophila* neuromuscular junctions can be viewed as electron dense T-Bars where

synaptic vesicles cluster (Figure 1.2) while in the frog NMJ it takes the shape of "beams and ribs". The proteins forming the active zone cytomatrix can be divided into three groups: (a) **cytoskeletal proteins**, such as actin, tubulin, and myosin; (b) **scaffolding proteins**, for example, CASK; and (c) **active zone specific proteins** like BRP, Basoon, RIM1 and many others. The primary function of this cytomatrix is to mediate the docking and trafficking of synaptic vesicles. The synaptic vesicles cluster, tether and fuse in the active zone, thereby restricting the neurotransmitter release to only these regions. This spatial organization of the active zone allows precise regulation for transmission of the electrical signal between the sending and receiving neuron. [1-6].

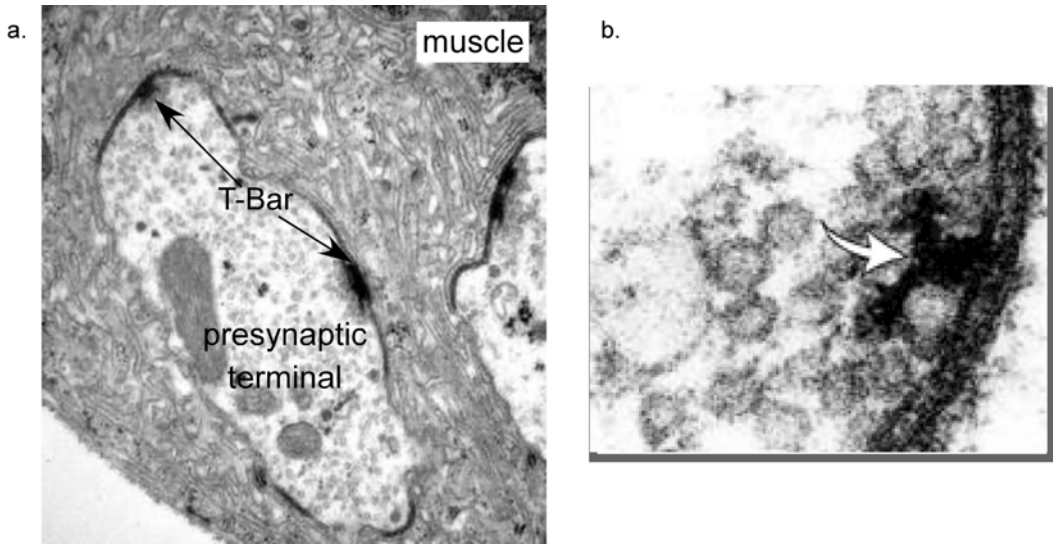

Figure 1.2: Electron Micrograph of *Drosophila* Larva Neuromuscular Junction. (a) The presynaptic terminal of a motor neuron is surrounded by muscle fibers on all sides. Electron dense structures called T-Bars. are observed at the junction of the nerve and the muscles. (b) The T-Bars represent the active zone, the region where the vesicles cluster, tether and fuse at the presynaptic terminal. The spherical vesicles can be observed around the T-Bar. Figure modified from *Atwood, 2006* [1].

1.3 **Synaptic Vesicle Trafficking**

1.3.1 Fusion of Synaptic Vesicles

How synaptic vesicles are formed remains debatable [7], however, the classical model of vesicle fusion predicts that intracellular vesicle formation involves the budding of vesicles from endosomes. These vesicles, after being formed, accumulate in the presynaptic terminal. Neurotransmitter release occurs through a multi-stage process that includes docking, priming and fusion. The first step is docking, which involves physical attachment of the neurotransmitter filled vesicles to the active zones. After docking, SVs are primed to prepare for fusion. Next, the SVs fuse with the plasma membrane resulting in neurotransmitter release [8] (Figure 1.3).

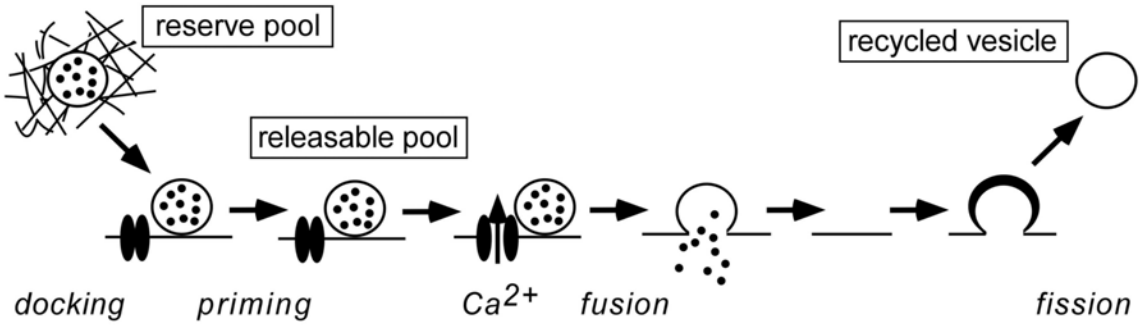

Figure 1.3: Steps in Synaptic Vesicle Fusion. Vesicle fusion is a multistage process that includes docking, priming, fusion and recycling.

1.3.2 Vesicle Recycling: Classical Endocytosis and Kiss and Run

Endocytosis and recycling follow vesicle fusion to maintain the synaptic vesicle pool at the synaptic terminal. SV can be retrieved from the plasma membrane through classical clathrin-mediated endocytosis, as observed during endocytosis in other cellular systems [9-11]. According to this classical model, SV collapse into the plasma membrane is followed by the assembly and endocytosis of clathrin coated vesicles. Adapter proteins recruit clathrin to the plasma membrane; this causes plasma membrane to invaginate and finally pinch off to form vesicles in a dynamin dependent manner (Figure 1.4).

An alternate model for vesicle fusion, called 'Kiss and Run' has been proposed to mediate rapid recapture of synaptic vesicles during high frequency stimulation [12, 13]. This model predicts that vesicles release neurotransmitter through a narrow pore that transiently connects the vesicle interior to the extracellular space. These vesicles are then retrieved intact into the active zone without allowing complete mixing of vesicle and plasma membrane. After the pore closes, vesicles detach from the active zone. Kiss and run appears to be the dominant mode of recycling during high frequency stimulation, although this is controversial [14, 15]. It is possible that both the processes occur during high frequency stimulation (Figure 1.4).

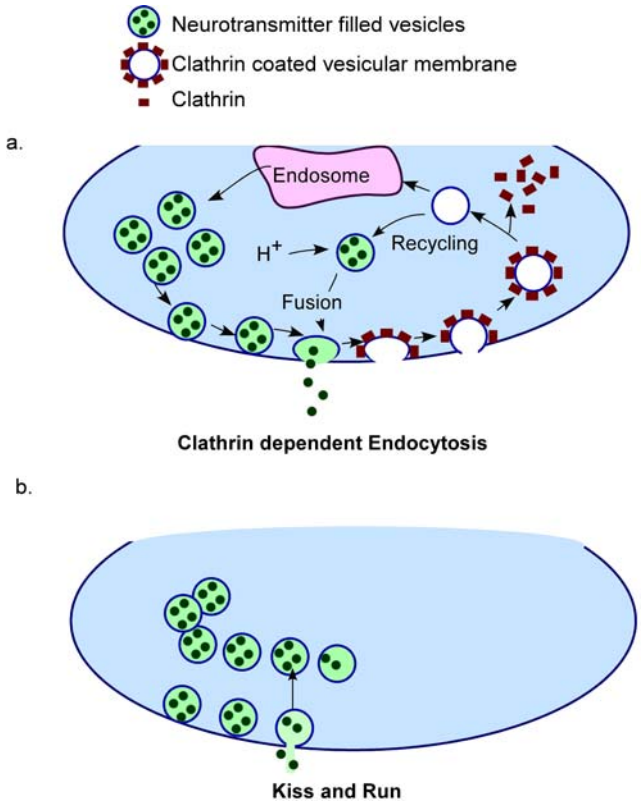

Figure 1.4: Two Models for Endocytosis. (a) Clathrin dependent Endocytosis model, which predicts vesicle recycling clathrin coated intermediates, and (b) Kiss and Run model, which envisage vesicles fusing briefly with the plasma membrane to release their contents.

1.3.3 Synaptic Vesicle Pools

Under resting conditions, a small percentage of the vesicles are docked to the plasma membrane while the majority of vesicles form a homogeneous population distributed in the presynaptic terminal. Despite the absence of any visible segregation of vesicles, synaptic vesicles can be grouped into three different classes based on their functions: (a) the readily releasable pool (RRP), (b) the recycling pool, and (c) the reserve

pool [16, 17] (Figure 1.5). Vesicles that are available immediately for fast fusion in response to a stimulus form the readily releasable pool. These vesicles are docked and primed to the active zone. Note that not all docked vesicles are necessarily immediately releasable. The second pool of vesicles, the recycling pool, maintains release on moderate physiological stimulation. They constitute 5-20% of the total pool population. The reserve pool is thought to be the depot of synaptic vesicles from which release is triggered only during intense stimulation. The RRP, being attached to the active zone, does not need to be mobilized in response to stimulation. In contrast, the recycling and the reserve pools are not present in the active zone and hence need to be moved for exocytosis to occur. The mobilization of vesicles can occur through random diffusion or directed movement with the help of cytoskeletal 'tracks'.

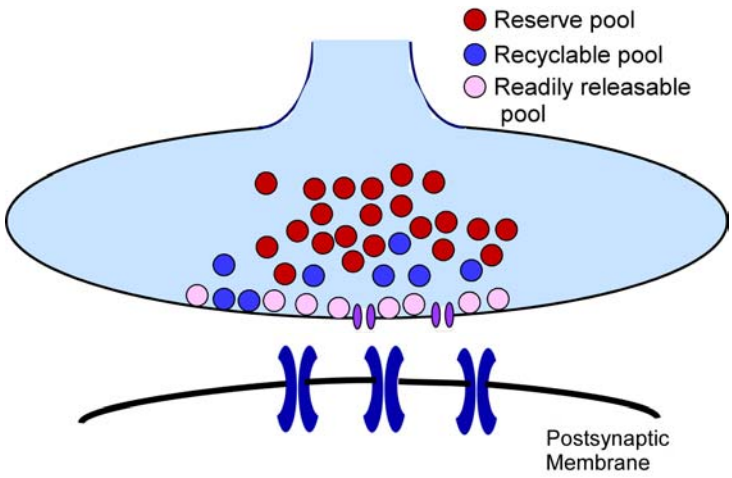

Figure 1.5: Three Vesicle Pools. The vesicle can be functionally grouped into three groups: readily releasable pool (RRP), recycling pool and reserve pool. The RRP is available for immediate use, the recycling pool is used during normal physiological stimulation and the reserve pool forms the depot of vesicles. These pools, however, can be segregated visually.

1.3.4 Core Proteins in Synaptic Vesicle Fusion

Precise regulation of vesicle fusion and exocytosis is required to maintain the efficacy of synaptic transmission. This regulation is brought about by a myriad of proteins, of which **SNARE** family and its interacting proteins are key components. SNARE proteins are thought to be the minimal machinery that can drive membrane fusion [18].

The SNARE proteins consist of a set of three membrane proteins: **synaptobrevin**, a vesicle associated membrane protein, and two plasma membrane associated proteins, **syntaxin**, and **SNAP-25** (Synaptosome Associated Protein of 25 KDa) . The SNARE proteins were discovered through molecular and biochemical analyses of components that were essential for reconstitution of vesicle fusion in a cell free system. The SNARE proteins were identified as membrane receptors for SNAP (Soluble NSF Attachment Protein) and NSF (N-Ethylmaleimide Sensitive Factor) and therefore designated as SNAREs (SNAp REceptor)[19-21].

Synaptobrevin is present in the vesicle membrane and is called vesicle SNARE (v-SNARE) while the plasma membrane associated syntaxin and SNAP-25 are called target-SNAREs (t- SNARE) [20, 22] (Figure 1.6). During priming, the v- and t- SNAREs bind loosely to each other to form the “pre-fusion” intermediate referred to as a trans-SNARE complex. The fusion is complete when the fusion pore opens upon merging of the vesicular and presynaptic plasma membranes. The three SNARE proteins form a bundle of four α-helices. SNARE complexes formed by coiled-coil interaction of α-

helices of the proteins which acts downstream of vesicle docking. The energy derived from the SNARE complex assembly drives the membrane fusion for exocytosis [23].

The SNARE complex is disassembled after fusion and the vesicle membrane is endocytosed to maintain the vesicle pool within the presynapse. The disassembly of SNARE complex requires considerably high metabolic energy, which is provided by an ATPase called NSF (*N*-ethylmaleimide sensitive fusion protein). NSF does not interact on its own with the complex, but requires cofactors known as SNAPs. This disassembly resets the SNARE protein for another round of docking and fusion [24, 25].

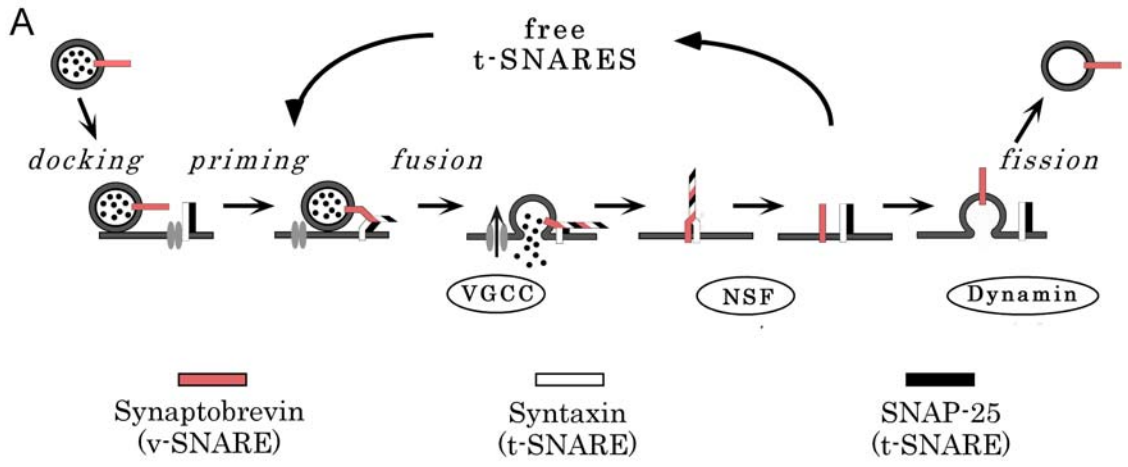

Figure 1.6: Core Proteins in Synaptic Vesicle Fusion. In the presynaptic terminal, vesicles are brought from the reserve pool and dock to the plasma membrane. The vesicles are primed by the binding of SNARE vesicle protein (v-SNARE) with two plasma membrane (target) proteins (t-SNARE), syntaxin and SNAP-25. Primed vesicles are available for fusion in response to calcium entry. When an action potential arrives at the presynaptic terminal, membrane depolarization activates voltage-gated calcium channels (VGCC) and the resulting influx of calcium triggers synaptic vesicle fusion and neurotransmitter release. After fusion, N-ethylmaleimide sensitive factor (NSF) disassembles SNARE complexes and releases syntaxin and SNAP 25 for subsequent vesicle priming. Vesicles are recycled via endocytosis mediated by dynamin and other proteins.

Numerous SNARE interacting proteins like c**omplexin, synapsin**, and **synaptophilin** present in the synaptic terminal regulate the efficacy and strength of neurotransmission by modulating SNARE complex formation (Figure 1.6). The **Sec1/Munc-18 (SM)** protein family confers specificity to SNARE dependent trafficking [26, 27]. Although the exact role of SM proteins is not clear, there is evidence suggesting that they act by binding syntaxin. It appears that the SM gene products vary in their mode of action in different systems [8, 28-30].

1.4 Presynaptic Voltage Gated Calcium Channels

Calcium channels play a critical role in neurotransmitter release. The conversion of an electrical signal to a chemical message requires calcium influx through voltage gated calcium channels. The calcium ions act like a "second messenger" by coupling the membrane potential to neurotransmitter release. The calcium influx needs to be tightly coupled to the release process of neurotransmitters such that presynaptic calcium entry is followed by neurotransmitter release and postsynaptic response on a millisecond time scale. The voltage dependence, selective permeability to calcium ions and localization in the active zone (the neurotransmitter release site) facilitate precise spatio-temporal regulation of neurotransmitter release by the calcium channels.

The intracellular concentration of calcium is very low (~100nM) compared to other alkali metals like sodium and potassium, which are present in the mM range. The low $[Ca]_i$ serves an advantage to cellular signaling; a relatively small influx of calcium ions, causes a significant change in intracellular calcium concentration so as to deliver an

ion-encoded message. The Ca^{2+} ions, thus, act as a key signal transducer, like G-protein coupled receptors or other famous membrane associated signal transducers (Figure 1.7). The opening of voltage-gated calcium channels rapidly raises the local calcium concentration by allowing Ca^{2+} to enter the cell. The calcium influx acts as a diffusible second messenger [31].

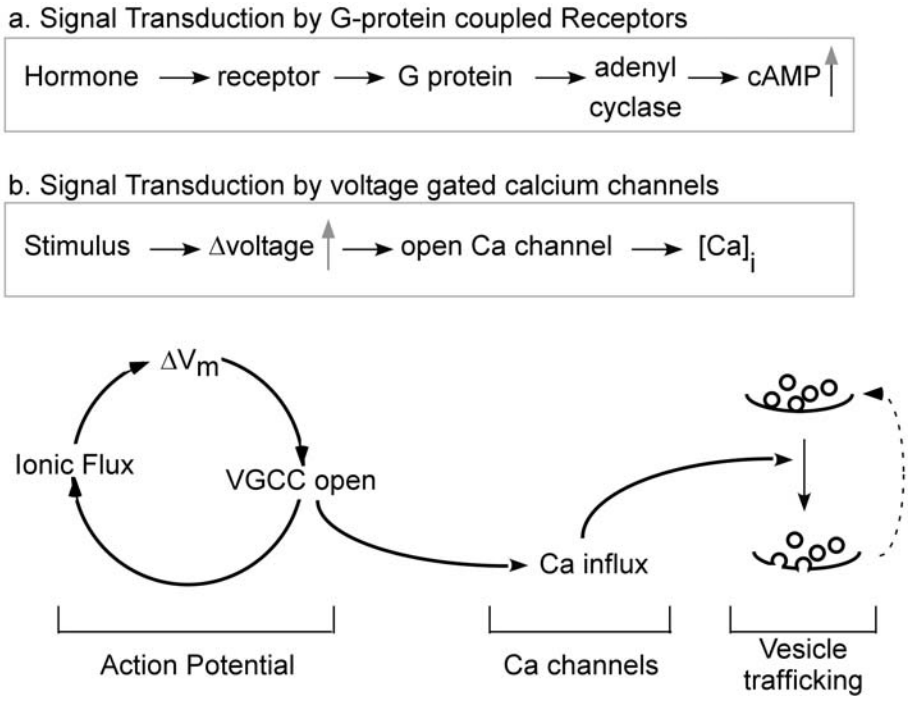

Figure 1.7: Calcium Channels as Key Signal Transducers at the Synapse. Ca channels can be modeled as key signal transducers analogous to other membrane associated signaling systems, as for example, G-protein coupled receptors. In this pathway, a stimulus causes to generate action potential, which in turn, causes membrane depolarization. Depolraization leads to the opening of voltage gated calcium channel. The Ca influx increases intracellular calcium concentration. Thus, Ca acts as a diffusible second messenger and triggers the cellular event, vesicle fusion (Adopted from Zamponi, 2005 [31].

VGCCs are heteromultimers composed of four or five subunits: the primary α_1 subunit and the auxiliary β, $\alpha_2\delta$ and possibly a γ subunit (Figure 1.8). Nine types of neuronal voltage gated Ca^{2+} channels have been identified through their distinct biophysical and pharmacological properties: L, N, P, Q, R and T-type Ca channels [32]. N and P/Q-type channels are the main channel subtypes located in the presynaptic terminals where their opening is linked to neurotransmitter release. The diversity of calcium channel is attributed by the presence of different isoforms of α_1 subunit as well as the auxiliary subunits [33].

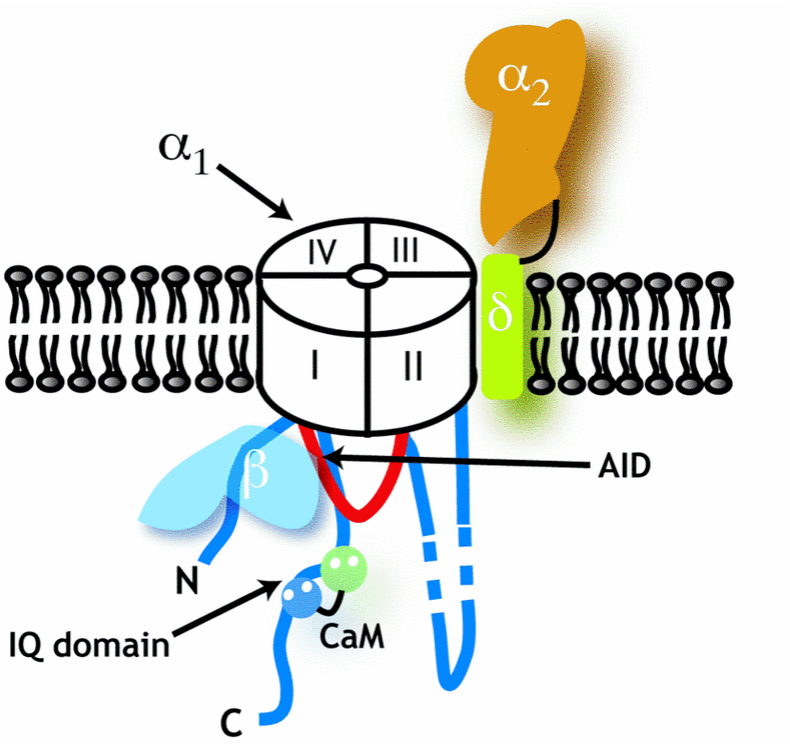

Figure 1.8: Voltage Gated Calcium Channel (VGCC). The VGCCs are heteromultimers composed of four or five subunits: the primary α_1 subunit and the auxiliary β, $\alpha_2\delta$ and possibly a γ subunit. The α_1 subunit is composed of four domains I-IV. The AID or the alpha1 interacting domain is the site of interaction between α_1 and β subunit. Figure modified from Petegam, 2006 [34].

1.4.1 α_1 Subunit of Voltage Gated Calcium Channels

The α_1 subunit, the primary structural subunit of the channel complex, forms the conduction pore, voltage sensor and gating apparatus. This subunit is comprised of four homologous domains (I-IV), each of which contains six transmembrane segments (S1 to S6) and a membrane associated "P" loop between S5 and S6. The S5, S6 and P-loop form the channel pore through which the Ca ions enter [35]. The S4 segment contains several positively charged amino acids and acts as a voltage sensor. Upon depolarization, the S4 segment undergoes conformational change, leading to opening of the channel pore. The amino acid sequence of the S4-S6 segment of the subunit is highly conserved, indicating its importance in the channel function [36].

The four domains (I-IV) are connected by three intracellular loops (called I-II, II-III and III-IV loops) [33], which along with the cytoplasmic N and C terminal, serve as sites for interaction of several proteins involved in channel regulation. These domains interact with a number of protein complexes and modulate calcium channel activity [37]. For instance, the IQ motif of the intracellular C-terminus interacts with Ca^{2+}/Calmodulin and influences calcium dependent inactivation/facilitation properties of the channel [38] (Figure 1.9) .

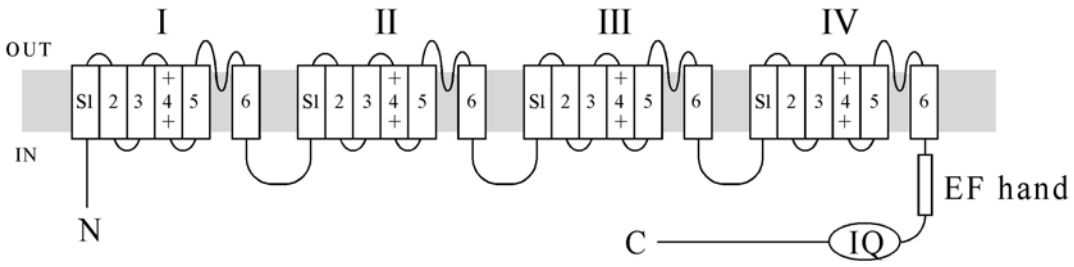

Figure 1.9: Topology of α_1 Subunit of Calcium Channel. Roman numerals refer to the four repeating domains, each consisting of six transmembrane segments (S1-S6). The charged S4 segment is thought to act as a voltage sensor. Both the N and C termini are intracellular. The calcium binding domain (EF hand) and the calcium calmodulin binding domain (IQ) are present within the C-terminal cytoplasmic domain.

1.4.2 **The Auxiliary Subunits of Voltage Gated Calcium channel**

1.4.2.1 β Subunit

The auxiliary β subunit is an intracellular hydrophilic protein associated with the α_1 subunit. The β subunit binds to a specific sequence of the intracellular I-II linker of the α_1 subunit called the AID (α_1 interaction domain). A 41 amino acid sequence (BID) has also been identified as the minimal sequence required to bind to the α_1 subunit [39]. The α_1 and β subunits are thought to bind with a 1:1 stochiometry in heterologous systems, however, it remains to be determined whether this is always the case for native calcium channels [34, 40]. The β subunit plays an important role in trafficking and expression of functional calcium channels in the plasma membrane. It also plays an important role in determining the biophysical properties of the channel; it hyperpolarizes

the voltage dependence of activation of all VGCCs (smaller change in ΔV_m causes the channel to open). There are several phosphorylation sites in the β subunit that can be phosophorylated by protein kinases, which, in turn, control channel function. With all these roles, the β subunit appears to be more than a passive structural component of the calcium channels [41, 42].

1.4.2.2 $\alpha_2\delta$ Subunit

The auxiliary α_2 subunit is an extracellular membrane protein connected to the transmembrane δ subunit through disulphide linkage. A single gene encodes both the α_2 and δ subunits. The gene product undergoes post translational cleavage and the C-terminal of the pro-protein forms the δ subunit. Both subunits are highly glycosylated and have extracellular N-termini. The $\alpha_2\delta$ subunit increases the density of the VGCCs in the plasma membrane. It is also the target for important therapeutic drugs and mutation in $\alpha_2\delta$ genes have been implicated in several diseases such as cerebral ataxia and epilepsy [43].

1.4.3 Calcium Channel Regulatory Proteins

Calcium Binding Proteins

Calcium influx through the voltage gated calcium channels can inactivate or facilitate the channels by feedback mechanism, thereby causing calcium dependent inactivation (CDI) and calcium dependent facilitation (CDF), respectively. A calcium

sensor molecule called calmodulin mediates both CDI and CDF. Calmodulin binds to the IQ motif of the C-terminal cytoplasmic tail of α_1 subunit. Calmodulin (CaM), a calcium sensor, is constitutively associated with the calcium channel [38],and can thus sense fluctuations caused by calcium entry through the channels. The calmodulin molecule has two N-terminal Ca^{2+} binding sites and two C-terminal binding sites for calcium. Local Ca^{2+} influx (characterized by intense, spike-like Ca^{2+} fluctuations) through a channel drives preferential binding of calcium to the C-terminal lobe of the resident CaM that is attached to the channel [44]. In contrast, global elevation of calcium concentration, caused by calcium influx through an ensemble of channels, results in calcium binding to the N-terminal sites. In N and P/Q type of channels, calcium binding to the N-terminal site induces conformational change in CaM triggering CDI. Conversely, CDF is induced upon calcium binding to the C- terminal lobe. CDF is not found in N-type channels, but is unique to P/Q-type channels. Calmodulin, thus, acts as a "molecular switch" between inhibitory and stimulatory regulation. Relative contribution towards CDI and CDF, in turn, is regulated by the alternate splicing of calcium channel mRNAs and the total number of active calcium channels present in the membrane [32]. Other calcium binding proteins like calcium binding protein 1 (CaBP1) and visin-like protein 2 (VILIP2) also regulate the calcium channel activity.

SNARE proteins

Presynaptic calcium channels are thought to interact directly with the SNARE proteins (synaptobrevin, SNAP-25 and syntaxin), which are core proteins required for synaptic vesicle fusion. The molecular link between calcium channel and

exocytotic machinery guarantees that vesicle fusion occurs within a restricted zone where appropriate calcium concentration is attained upon calcium channel activation. Synaptotagmin I, a calcium sensor, interacts with both the calcium channel and the SNARE complex and is thought to mediate calcium dependency of the release process [45]. A particular sequence present in the interdomain linker II-III of the calcium channel, called the SYNPRINT domain appears to be the site of interaction of these proteins with the calcium channel. However, this sequence is not found in all organisms, for example, the SYNPRINT domain is absent in the *Drosophila* presynaptic calcium channel α_1 subunit [46]. Given the primary role of the α_1 subunit in neurotransmitter release, it is possible that a novel interaction domain exists or there is an alternate mechanism for fast coupling of calcium influx and vesicle fusion .

1.5 *Drosophila melanogaster* as a Model System for *in vivo* Analysis of Synaptic Transmission

Neurotransmitter release is highly conserved in evolution. Despite the dramatic differences in complexity between *Drosophila,* mice and humans; the key neuronal proteins and the basic mechanisms of neuronal function are remarkably similar. Over the past century, *Drosophila* has emerged as a powerful tool for studying cellular and molecular mechanisms of neurotransmission [47]. The Drosophila nervous system is simple compared to mammals, but complex enough to display many complicated and intricate behaviors, such as learning and memory.

A relatively short life span and the ease of culturing in the laboratory make flies an alluring model system. Fly genetics is well understood and the combination of molecular, genetic, and genomic techniques that can be applied on *Drosophila* make it a powerful model system. Introduction of random mutations anywhere in the genome, P-element mediated transgenesis, the UAS-Gal4 system (a tool for *in vivo* gene over expression) and the *flp-FRT* system (a site specific recombination mapping system), are just a few of these approaches .The complete sequencing of the fly genome has assisted in gaining further insight into fly genetics through genomic and proteomic analysis. Analysis of the proteins predicted from the fly genome has revealed an extensive conservation of many proteins involved in vesicle trafficking [48, 49].

1.6 Temperature Sensitive (TS) Mutants in *Drosophila*

Mutations have been introduced in fruit flies to alter various aspects of nervous system functions. Mutations can be easily produced in *Drosophila*. Alteration of a specific gene, for example, a gene responsible for calcium channel α_1 subunit, could be employed to see how it affects the neurotransmitter release process. Alternately, random mutations can be introduced in the flies by irradiation, P-element transposon mobilization or chemical mutagens such as ethyl methane sulphonate (EMS). The mutants can be screened for neuronal defects such behavioral or physiological defects, followed by identification of the genes that functions in a given process. Identification of conditional mutants has been particularly useful in this approach. The temperature sensitive (TS) paralytic mutants have been used extensively in studying the neuronal functions. The

advantage of TS paralytic mutants is that a gene product may be turned on or off rapidly at will. These mutants exhibit wild-type behavior at permissive temperature (18-25^{o}C) but paralyze rapidly in seconds or minutes when exposed to elevated temperature (like 36^{o}C) [50]. Normal mobility is regained after return to the permissive temperature. Elevated temperature is thought to induce acute disruption of a specific gene product at synapses *in vivo.* The acute reversible perturbation of a gene product reduces or eliminates the challenge of long term compensation owing to presence of a disruptive mutated product during development. To summarize, TS mutants provide conditional, temporal control of assaying protein function *in vivo* [51]. The rate at which the TS mutants paralyze is dependent on the temporal requirement of the gene product.

1.7 Discovery and Characterization of a TS Paralytic Mutant of a Presynaptic Calcium Channel (*cac^{TS2}*)

Benzer and Siddiqi isolated several alleles of a TS paralytic mutant called *comatose* [52, 53], which was later found to be a TS mutant of the *dNSF1* gene [54-56]. To identify a modifier of *comatose,* a genetic screen was performed in our laboratory [57]. The screen recovered *cac^{TS2}*, a TS paralytic mutant of *cacophony.* This gene codes for the α_1 subunit of voltage gated calcium channels.

The *cac*^{TS2} mutation is recessive, and found at amino acid site 1385 where serine substituted for proline (P1385S) Figure 1.10. The proline 1385 is a part of the highly conserved proline pair adjacent to the EF hand of α_1 subunit of VGCC [58]. It is possible that this mutation at proline 1385 affects the folding transitions of α_1 subunit C-terminus, which have been shown to be connected to channel activity.

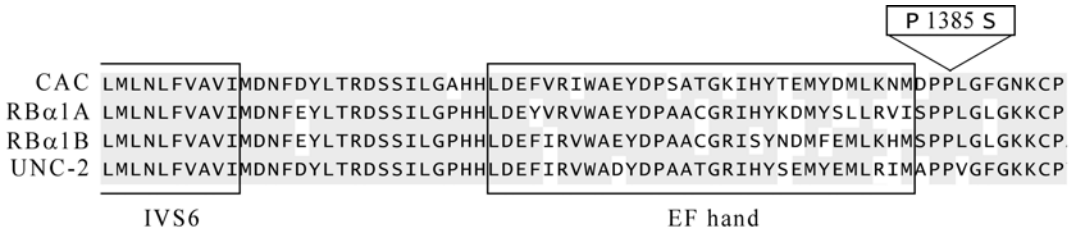

Figure 1.10: The *cac*^{TS2} mutation. Alignment of CAC with related calcium-channel a1 subunit polypeptide sequences is shown. Amino acid identities with CAC are shaded. Boxed sequences correspond to the EF hand and a portion of the IVS6 transmembrane segment. The cacTS2 mutation, P1385S, maps to an invariant proline residue adjacent to the EF hand. The aligned sequences correspond to CAC, rat brain α_1A and α_1B and C.elegans UNC-2, respectively [58].

The *cac* locus was initially identified in a genetic screen for altered courtship song; in fact, this was the first single gene isolated based on altered courtship song . Kulkarni et al mapped the *cac* allele to the X-chromosome [59, 60]. Later, sequencing of the α_1 subunit of voltage gated calcium channels led to the identification of the *cac* locus [61].

The *cac*^{TS2} mutants exhibited wild-type behavior at room temperature, whereas, their motor function was affected at restrictive temperatures. The mutants displayed spinning behavior and lack of co-ordination at 36^{o}C, while at 38^{o}C, they rapidly paralyzed. The synaptic phenotype was examined at the neuromuscular junctions of the dorsal longitudinal flight muscles (DLM) of the adult flies and revealed wild-type synaptic currents at 20^{o}C. In contrast, exposure to elevated temperature produced a marked decrease in the amplitude of the current with respect to wild type [46]. The extent of current reduction was dependent on the temperature (Figure 1.11).

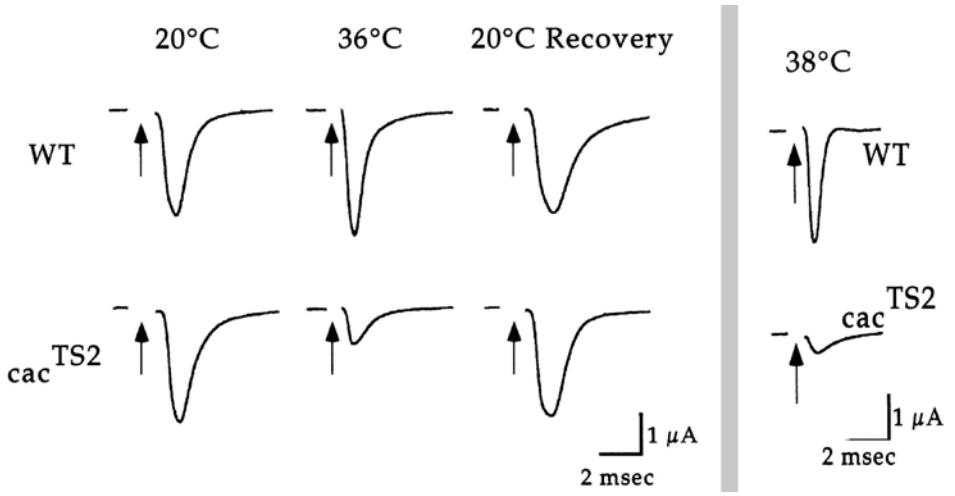

Figure 1.11: Synaptic Physiology of cacTS2 mutant. Representative Excitatory Postsynaptic Current (EPSC) recordings from dorsal longitudinal flight muscle (DLM) neuromuscular synapses of wild type (WT) and cac^{TS2} at 20°C and 36°C. cac^{TS2} exhibits a wild-type EPSC amplitude at 20°C. At the restrictive temperature of 36°C, the EPSC amplitude is significantly reduced relative to WT. This change is reversible; the EPSC amplitude recovers when the temperature is brought back to 20°C. The extent of current reduction was dependent on the temperature, at 38°C; the EPSC amplitude was further reduced in comparison to 36°C. Stimulation artifacts were removed for clarity. All recordings were performed on flies reared at 20°C. *Modified from Kawasaki, 2000[46]*.

1.8 Modifier Screen for cac^{TS2} Paralytic Phenotype

The cac^{TS2} mutant has also served as a starting point for further genetic analysis. Previous work on isolation of genetic modifiers of cac^{TS2} has identified several TS paralytic mutants with distinct synaptic phenotypes at elevated temperature. The first screen isolated four intragenic modifiers and six extragenic modifiers on X-chromosome [62]. Among the six extragenic modifiers, one was allelic to *shibire*, three fell in the locus of *futsch* and two others remains unidentified (Unpublished data, obtained from personal communication with Dr. B. Zou).

1.9 Genetic Screen for Second Chromosome Modifiers of *cac^{TS2}* Paralytic Phenotype

To expand the knowledge on the functions and interactions of *cac*-encoded calcium channels, a screen for second chromosome genetic modifiers of the *cac*^{TS2} paralytic phenotype was initiated. This dissertation aimed at identifying and genetically characterizing second chromosome modifiers of *cac*^{TS2} TS paralytic phenotype. Mutations in genes that can modify the *cac^{TS2}* paralytic and synaptic phenotype are potential candidates of the molecular machinery governing the synaptic transmission. They can also interact with the presynaptic calcium channel and thus shed light on molecular mechanisms of calcium channel function.

Two enhancers have been identified in the genetic screen and they have been genetically mapped to 54D4-D5 cytological units in the second chromosome. The mutants recovered in this screen are valuable. They are either novel TS alleles of previously characterized genes or may identify new members of the molecular machinery governing the synaptic transmission. Further analysis will reveal the gene involved in the enhancement of TS paralytic phenotype of *cac^{TS2}* and thus, further elucidate the *in vivo* roles of specific gene products in synaptic transmission.

Chapter 2

GENETIC SCREEN TO IDENTIFY SECOND CHROMOSOME MODIFIERS OF cac^{TS2} MUTANTS IN *DROSOPHILA*

2.1 Overview

A genetic screen to identify mutations that alter the TS paralytic phenotype of *cac*^{TS2} is the basis of this study. As mentioned previously, the *cac*^{TS2} mutants exhibit distinct behavioral phenotypes at 36^{o}C and 38^{o}C. At 36^{o}C, the mutants display motor dysfunctions, but do not paralyze for >50 minutes. At 38^{o}C, the flies paralyze in approximately 20 seconds. A potential enhancer of *cac*^{TS2} can augment the TS phenotype by causing rapid paralysis at 36^{o}C. Conversely, suppression of *cac*^{TS2} phenotype could alleviate the severe motor defects observed at 36^{o}C. In this chapter the genetic screen conducted to identify the second chromosome modifiers and the TS paralytic and synaptic phenotype characterization have been described.

2.2 Materials and Methods

Drosophila Stocks

The fly stocks (i) *w cac^{TS2}; Iso2*, (ii) *w cac^{TS2}; Sco / CyO,GFP,* and (iii) *w; Sco / CyO,GFP* were from our laboratory stock. Wild-type flies were Canton S. The stocks were maintained at 20°C or at room temperature (~23°C).

Mutagenesis

One to three day old *cac*^{TS2} males with isogenized second chromosome were exposed to a mutagen, ethylmethane sulphonate (EMS). These males, maintained at room temperature (~22°C), were separated from females for 24 hours, starved for three hours and finally exposed for 24 hours to 25mM EMS dissolved in a 1% sucrose solution (Dellinger et al, 2000). Mutagenized males were mated in groups of 30 with 30-40 *cac*^{TS2} females carrying the visible second chromosome marker, *Scutoid* (*Sco*), in *trans* to a *Curly of Oster* (*CyO*) balancer chromosome carrying a GFP transgene marked with w^+ (Figure 2.1). The EMS treated flies were discarded 5 days after mating to maximize the percentage of uniquely mutated chromosomes. The mutagen affects the gonial stem cells as well as the mature sperm. Sperm requires ~5 days to mature after gonial cell division, producing multiple sperms with identical mutations. Hence, the males were discarded to ensure the production of all independently induced unique mutations. This reduces wastage of time by preventing analysis of the same mutant allele more than once. All the F_1 male progeny produced should carry a unique mutagenized second chromosome.

Individual F_1 male flies were backcrossed to F_0 females. This was done to screen each of the uniquely produced mutagenized second chromosomes separately. After mating of F_2 heterozygous siblings, the F_3 flies isogenic for a mutagenized second chromosome in a cac^{TS2} background were screened for TS paralytic behavior. All the flies were reared at 23°C.

Behavioral analyses

For behavior analysis, the flies were placed in a vial maintained at 36°C by immersion in a preheated water bath. Two to three day old flies in groups of 3-6 were examined for any deviation from the cac^{TS2} behavioral phenotype at the same temperature. Lines that behaved unlike cac^{TS2} during the first test were tested 5 more times. Time for 50% paralysis represents the time at which 50% of the flies are no longer able to stand. Each test was 3 minutes in duration (Dellinger, 2000). For the screening, the flies were reared at room temperature.

Electrophysiology

Excitatory Postsynaptic Current (EPSC) recordings were obtained from dorsal longitudinal flight muscle (DLM) neuromuscular synapses of adult flies. The posterior dorsal mesothoracic nerve, through which the DLM motor axons project to the muscle, was stimulated. The 33°C and 36°C recordings were obtained 7 minutes after the temperature in the recording chamber reached the desired value. All recordings were performed on flies reared at 20°C. All the recordings were done in collaboration with Dr. Fumiko Kawasaki as described previously [54].

Data analysis

All graphing and statistical analyses were carried out using the software Microsoft Excel (Microsoft Corp., Seattle, WA). The percentage of F_2 lines that produced progeny was calculated by dividing the number of F_2 crosses producing progeny with the total number of F_2 lines set up. The lethality percentage was calculated by dividing the number of F_3 homozygous lines with that of F_2 lines that produced progeny. Data are presented as mean $\pm$ SEM. Statistical analyses were performed using paied t-test and p-value ≤ 0.05 were considered significant. In the figures, the values that varied significantly from the control are marked with asterisk.

2.3 Results and Discussions

2.3.1 A Screen for Second Chromosome genetic modifiers of *cac^{TS2}*

The *cac*^{TS2} paralytic phenotype is well suited for isolation of genetic modifiers. These mutants exhibit distinct behavioral phenotypes at 36^{o}C and 38^{o}C. At 36^{o}C, the mutants display motor dysfunctions, but do not paralyze for >50 minutes. At 38^{o}C, the flies paralyze in approximately 20 seconds. We predicted that a potential enhancer of *cac*^{TS2} would augment the TS phenotype by causing rapid paralysis at 36^{o}C. Conversely, suppression of *cac*^{TS2} phenotype could alleviate the severe motor defects observed at 36^{o}C.

The *cac*^{TS2} males with an isogenized second chromosome were exposed to the mutagen, ethylmethane sulphonate (EMS) for 24 hours. Mutagenized males were mated with *cac*^{TS2} females carrying the visible second chromosome marker, *Scutoid (Sco),* in *trans* to a *Curly of Oster (CyO)* balancer chromosome carrying a GFP transgene marked with w^+. The F_1 male flies were backcrossed to F_0 females. After mating F_2 heterozygous siblings, F_3 flies isogenic for a mutagenized second chromosome in a *cac*^{TS2} genetic background were screened for TS paralytic behavior at 36°C (Figure 2.1).

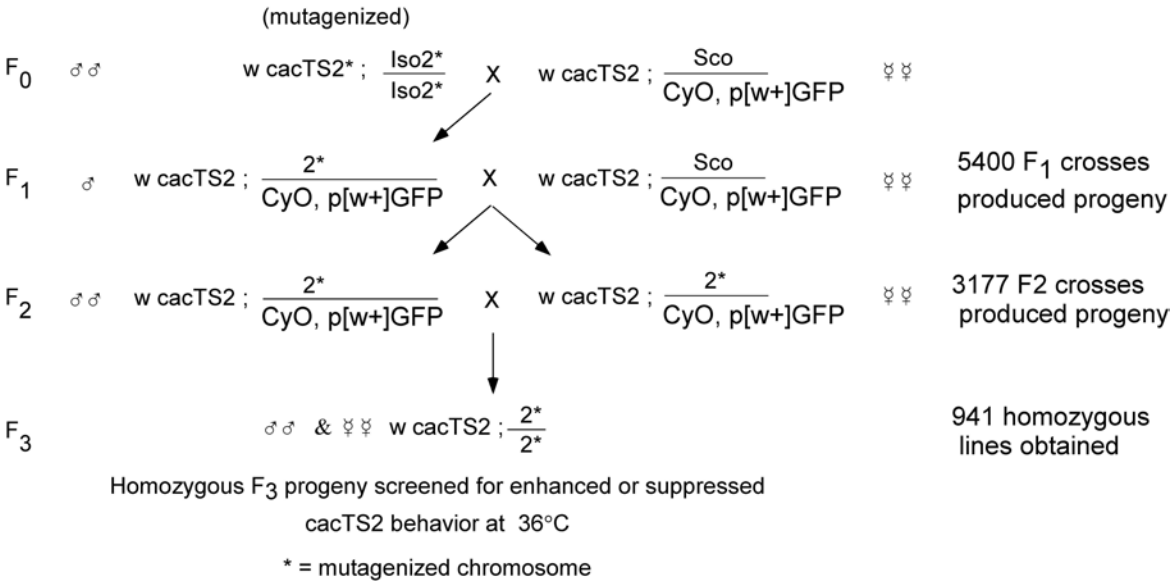

Figure 2.1: A F_3 Genetic Screen for modifiers of *cac*^{TS2}

In the present study, 4296 F_2 crosses were set up by mating the heterozygous siblings from 5400 F_1 lines. Out of the 4296 F_2 crosses, 3177 lines produced F_3 progeny. 31% of the 3177 F_2 lines (or 941 lines) that produced progeny were homozygous for the second chromosome. These 941 F_3 second chromosome homozygous flies in a *cac*^{TS2}

background were screened for alteration of behavior. The results are summarized in Figure 2.2. The lethality percentage for our screen was calculated to be 69 ± 1.31%. This is comparable to the reported frequency (80%) of second chromosome lethals after exposure to 25 mM EMS (Ashburner, 1989). The percentage of F_2 and F_3 progeny produced remained consistent over time (Figure 2.2) indicating that there was no procedural error involved in the process. Additionally, these values were also comparable to another F_3 screen for modifiers of cac^{TS2} carried out in our laboratory (data not shown). The consistency in these values indicates that the screen was performed systematically.

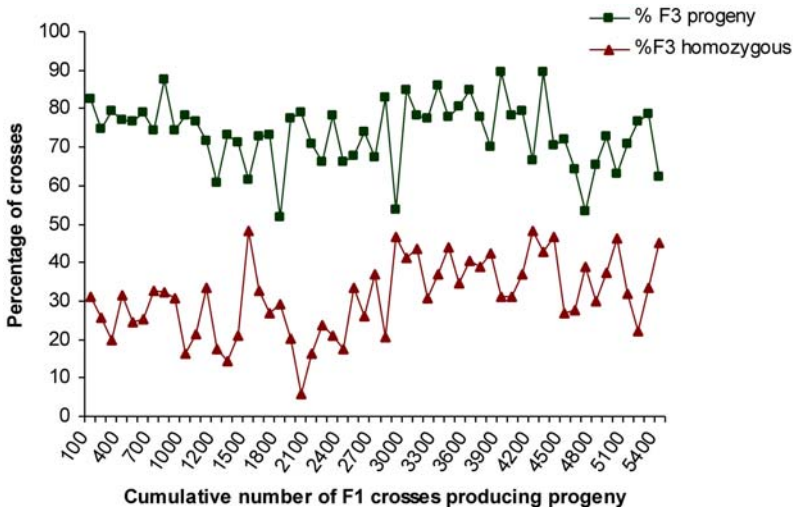

Figure 2.2: Overview of the Genetic Screen. Percentages of F_3 progeny produced in the F_3 screen were consistent over time. 5400 F_1 crosses were divided in groups of one hundred and the value for each group was plotted. Homozygous viable flies were screened for an enhanced or suppressed cac^{TS2} behavior phenotype at 36°C.

2.3.2 TS Paralytic Behavior of the Enhancers

We screened all the 941 homozygous lines for behavior analysis. These flies were reared at room temperature (22°C). After behavior analysis, 22 lines exhibited rapid TS paralysis (< 45 seconds) at 36°C, enhancing the *cac*^{TS2} phenotype. These lines were chosen for further analysis. Electrophysiological analysis was undertaken for the 23 lines exhibiting a consistent behavioral phenotype distinct from *cac*^{TS2} at 36°C.

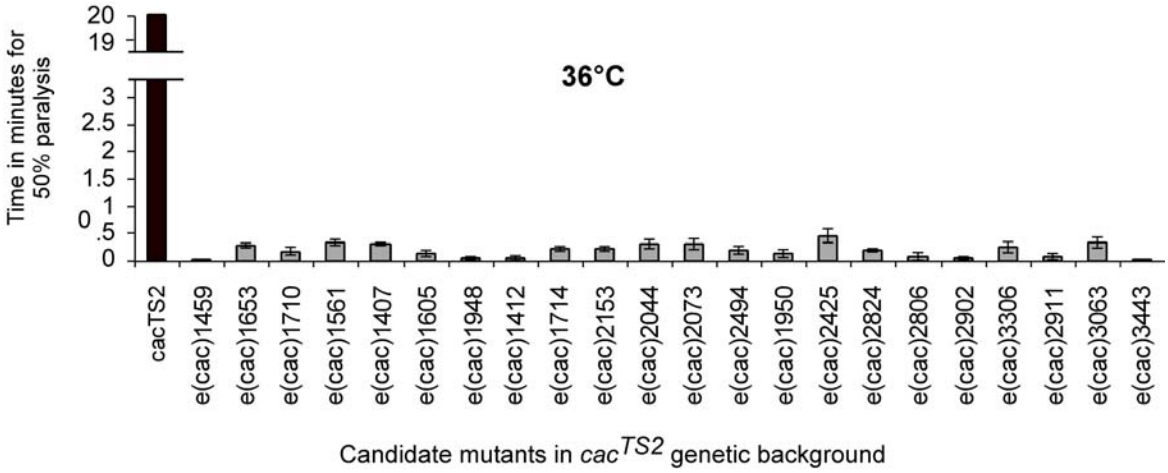

Figure 2.3: **TS Paralytic Behavior of Second Chromosome Enhancers of *cac*^{TS2}** (A) 22 candidate enhancers in the *cac*^{TS2} background exhibited rapid paralysis at 36°C, whereas *cac*^{TS2} alone does not paralyze at this temperature. *cac*^{TS2} behavioral tests were truncated after 20 min. All these lines were further examined for their synaptic physiology.

2.3.2.1 Recovery of Two Enhancers, e(cac)2902 and e(cac)3063, that have altered cac^{TS2} TS paralytic and synaptic phenotype

Two double mutants, *w cac*^{TS2}*; e(cac)2902* and *w cac*^{TS2}*; e(cac)3063* showed a marked TS decrease in the amplitude of the EPSCs in relation to *cac*^{TS2} (Figure 2.7). The TS paralytic behavior of these lines was thus retested with flies reared at 20°C

(Figure 2.4**).** Both the lines exhibited rapid paralysis at 36°C with a time for 50% paralysis of 0.02 and 0.09 minutes for *w* cac^{TS2}*; e(cac)2902* and *w* cac^{TS2}*; e(cac)3063* respectively. In contrast, cac^{TS2} alone did not paralyze at this temperature. cac^{TS2} behavioral tests were truncated after 20 min. Flies heterozygous for the enhancer mutation, *w* cac^{TS2}*; e(cac)2902/+* and *w* cac^{TS2}*; e(cac)3063/+* behaved like cac^{TS2} showing that both mutations are recessive.

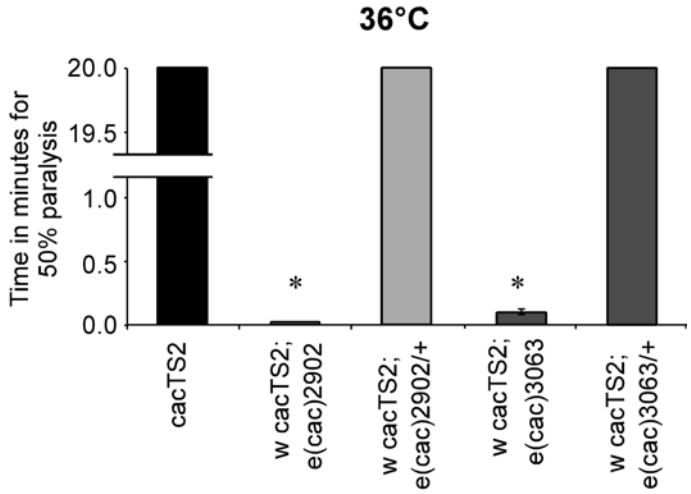

Figure 2.4: TS Paralytic Behavior of *e(cac)2902* and *e(cac)3063*. Two double mutants selected for further study, *w* cac^{TS2}*; e(cac)2902 and w* cac^{TS2}*; e(cac)3063* exhibit rapid paralysis at 36°C, whereas cac^{TS2} alone does not paralyze at this temperature. cac^{TS2} behavioral tests were truncated after 20 min. Flies heterozygous for the enhancer mutation, cac^{TS2}; e(cac)2902/+ and w cac^{TS2}; e(cac)3063/+, behaved like cacTS2 showing that both mutations are recessive. Asterisks mark values significantly different from control values.

2.3.3 Isolation of *e(cac)2902* and *e(cac)3063* from the cac^{TS2} Genetic Background

The two enhancer mutations, *e(cac)2902* and *e(cac)3063* were isolated from the cacTS2 mutation to investigate if the modifier mutation alone had any phenotype or not.

The scheme for isolating the mutation from *cac*^{TS2} genetic background is given in Figure 2.5.

The *e(cac)2902* heterozygous males were mated with *cac*^{TS2} females carrying the visible second chromosome marker, *Scutoid (Sco),* in *trans* to a *Curly of Oster (CyO)* balancer chromosome carrying GFP transgene marked with w^+. After mating F_2 heterozygous siblings, F_3 flies homozygous for *e(cac)2902* in a *white* genetic background were screened for TS paralytic behavior at 36°C and 38°C.

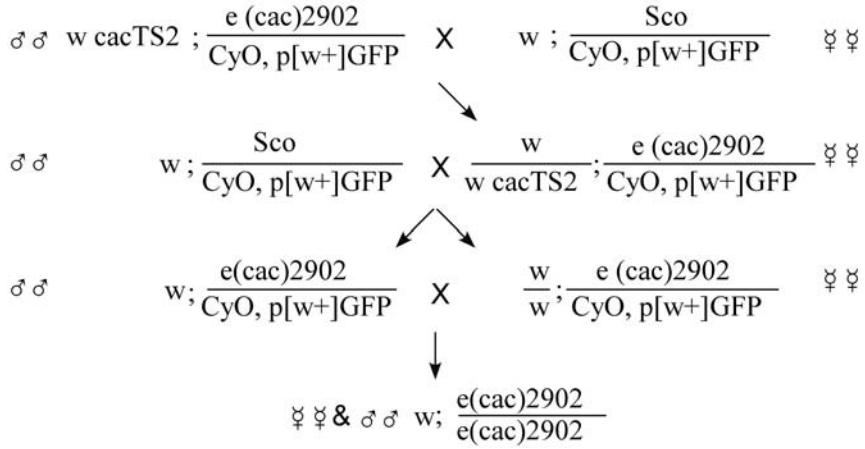

Figure 2.5: Scheme for Isolating the Enhancer Mutations from the *cacTS2* background.

2.3.3.1 TS Paralytic Behavior of e(cac)2902 and e(cac)3063 in Wild Type Background

Both *e(cac)2902* and *e(cac)3063* exhibited rapid TS paralysis at 38°C with times for 50% paralysis of 0.20±0.04 and 0.25±0.04 minutes, respectively (Figure 2.6), whereas wild-type (WT) did not paralyze for up to 20 minutes. This indicated that the

enhancer mutations alone produced TS paralytic behavior and the phenotypes of the two mutations were very similar.

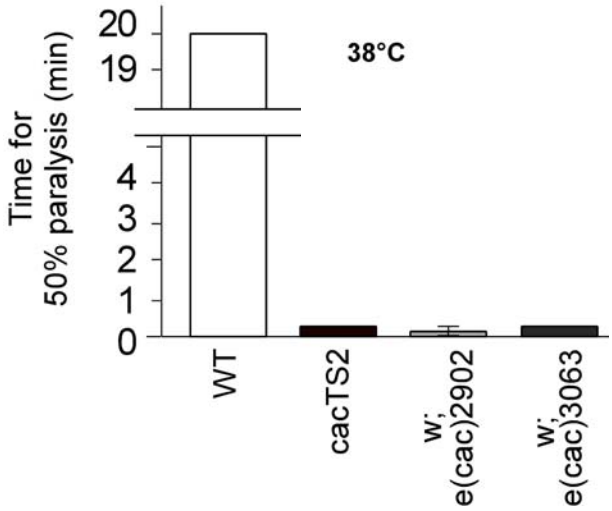

Figure 2.6: **TS Paralytic Behavior of *e(cac)2902* and *e(cac)3063*.** *w; e(cac)2902 and w; e(cac)3063* exhibit rapid paralysis at 38°C. WT behavioral tests were truncated after 20 min. Asterisks marks indicate significant difference.

2.3.3.2 e(cac)2902 and e(cac)3063 are Alleles of the Same Gene

The two enhancer mutations *e(cac)2902* and *e(cac)3063* were placed in *trans* to one another with cac^{TS2} in the background and tested for TS paralytic behavior at 36°C. The flies paralyzed immediately (result not shown), implying that *e(cac)2902* and *e(cac)3063* could not complement one another. This indicated that the two mutations fall within the same gene.

2.3.3.3 Synaptic Physiology of e(cac)2902 and e(cac)3063 in a cac^{TS2} or Wild-Type Genetic Background

Excitatory postsynaptic currents (EPSCs) were recorded from neuromuscular junctions of the dorsal longitudinal muscles (DLM) of adult flies by applying two-electrode voltage clamp. This technique prevents activation of postsynaptic voltage-gated ion channels and thus records the current passing through ligand-gated neurotransmitter receptor channels.

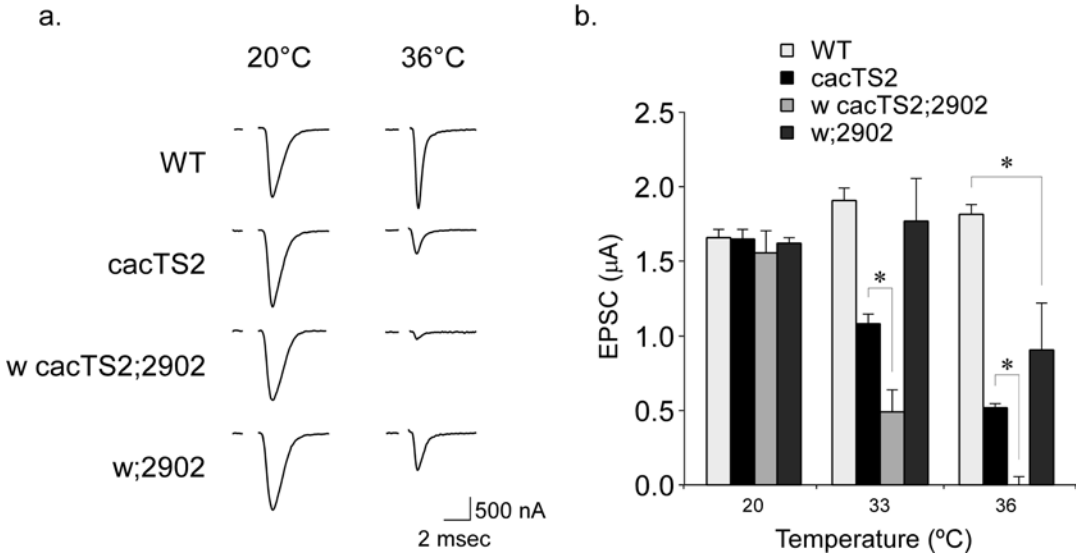

Figure 2.7: Synaptic Physiology of a Second Chromosome Enhancer of cacTS2. (A) Representative Excitatory Postsynaptic Current (EPSC) recordings from dorsal longitudinal flight muscle (DLM) neuromuscular synapses of wild type (WT), *cacTS2*, and the *w cacTS2; e(cac)2902* double mutant and *w; e(cac)2902* at 20°C and 36°C. *w cacTS2; e(cac)2902* and *w; e(cac)2902* exhibit a wild-type EPSC amplitude at 20°C. At the restrictive temperature of 36°C, the EPSC amplitude of *w cacTS2; e(cac)2902* is significantly reduced relative to both WT and cacTS2 alone. *w; e(cac)2902* amplitude is signicantly reduced compared to WT. Stimulation artifacts were removed for clarity. The 36°C recordings were obtained after 7 min at 36°C. All recordings were performed on flies reared at 20°C. (B) Mean EPSC amplitudes. SEM are represented by the error bars. Asterisks indicate the differences are statistically significant.

Recordings from double-mutant synapses were compared to those from *cac*^{TS2} at 20°C, 33°C and 36°C. As described previously, *cac*^{TS2} exhibited a wild-type synaptic current at 20°C and a marked reduction in the EPSC amplitude at 33°C and 36°C (Figure 2.7). Two candidate enhancers, *e(cac)2902* and *e(cac)3063*, in the presence of *cacTS2* in the genetic background, showed marked decrease in the EPSC amplitude of the EPSCs compared to *cac*^{TS2} alone (Figure 2.7 and Table 2.1). Systematic analysis was not done for *w cac*^{TS2}; *e(cac)3063* since complementation tests showed that *e(cac)2902* and *e(cac)*3063 were allelic. However, preliminary recordings suggested that the synaptic phenotype of *w cac*^{TS2}; *e(cac)3063* was very similar to that of *w cac*^{TS2}; *e(cac)2902* (data not shown). Synaptic current amplitudes recorded in WT, *cac*^{TS2} alone and *w cac*^{TS2}*; e(cac)2902* at 33°C and 36°C are indicated in Table 2.1. This indicated that the degree of enhancement of *cac*^{TS2} was dependent on the temperature.

Table 2.1: EPSC Amplitudes Recorded from DLM of TS paralytic Mutants at Permissive and Restrictive Temperature

	20°C *(n)*	**33°C *(n)***	**36°C*(n)***
CS	1.66±0.05μA *(24)*	1.91±0.08μA *(18)*	1.81±0.07μA *(9)*
***cac*^{TS2}**	1.65±0.05μA *(15)*	1.09±0.06μA *(11)*	0.51±0.03μA *(8)*
w cac*^{TS2}*; e(cac)2902	1.56±0.05μA *(5)*	0.49±0.15μA *(5)*	0.00±0.05μA *(3)*
w; e(cac)2902	1.62±0.05μA *(6)*	1.77±0.29μA *(5)*	0.91±0.31μA *(4)*

The mutation, *e(cac)2902,* when present in a wild-type genetic background, exhibited a synaptic phenotype distinct from wild-type at 36^{o}C, the EPSC amplitude of *w; e(cac)2902* was 0.91$\pm$0.31 μA in comparison to 1.81$\pm$0.07 μA observed in wild-type. These results indicate that *e(cac)2902* functions in synaptic transmission.

Chapter 3

GENETIC MAPPING OF THE ENHANCERS *e(cac)2902* AND *e(cac)3063*

3.1 Overview

The genetic screen led to the isolation of two second chromosome enhancers of cac^{TS2} phenotype, *e(cac)2902* and *e(cac)3063*. Genetic characterization was undertaken for the loci of these mutations to gain further insight on how these mutations affect cac^{TS2} function. Classical genetic mapping techniques were used for this purpose. This chapter describes the mapping techniques that led to the identification of the region containing the second chromosome mutation.

3.2 Materials and Methods

Fly Stocks

Meiotic mapping was done using our laboratory stock that contained the four visible markers, *Sternopleural (Sp), Scutoid (Sco), Lobed (L)* and *Pin*. The following chromosomal aberrations were obtained from the Bloomington Stock Center and used in deficiency mapping. Break points are indicated in parentheses: Df(2R)BSC49 (53D9;54B10); Df(2R)BSC44 (54B1;54B10); Df(2R)BSC161 (54B2;54B17); Df(2R)robl-c (54B17;54C4); Df(2R)k10408 (54C1;54C4) Df(2R)BSC45 (54C8;54E7);

Df(2R)14H10Y-53 (54D1;54E7); Df(2R)14H10W-35 (54E5;55B7); Df(2R)PC4 (55A;55F); Df(2R)P34 (55E2;56C11); Df(2R)BSC26 (56C4;56D10); Df(2R)BSC22 (56D7;56F12); Df(2R)AA21 (56F9;57D12); Df(2R)Exel7162 (56F11;56F16); Df(2R)BSC19 (56F12;57A4); Df(2R)02B10Y-14(54D6;54E8); Df(2R)14F06W-10(54D4;54D6); Df(2R)14F06Y-28(54D1-2;54D4); Df(2R)Exel7149, (54C10;54D5); Df(2R)Exel7150(54E1;54E9); Df (2L) FCK-20 (32D1; 32F1); Df (2R) CB21 (48E; 49A); Df (stan2) (46F1; 47B9); In(2)syt^{D27} (23B1) and Df (N6) (23A6;23B1).

Meiotic Mapping

In *Drosophila,* meiotic recombination occurs only in females. The relative position of the candidate gene can be estimated with respect to some known marker loci by studying the recombination frequency (RF) between the marker and the gene (Figure 3.1**)**. The higher the recombinant frequency between a marker and the candidate gene, the farther apart the two genes appear to be. The genetic map distance can be calculated using the following equation:

$$\text{Genetic Map Distance} = \frac{\text{Recombinants}}{\text{Recombinants + parentals}} \times 100$$

Conversely, a low frequency of recombination indicates close association between the gene and the marker. Male and female flies carrying the recombinant chromosome were screened for TS paralytic behavior at 36°C. Meiotic mapping employed four visible markers, *Sternopleural (Sp), Scutoid (Sco), Lobed (L)* and *Pin*.

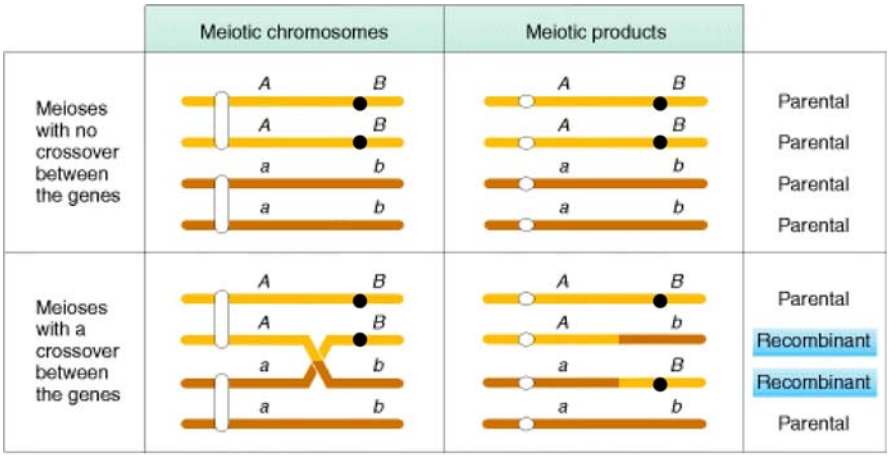

Figure 3.1: Recombinants arise from meioses in which nonsister chromatids cross over between the genes under study. *A* and *B* are two dominant mutations of *a* and *b* respectively. The black spot designate the mutation whose position is to be estimated relative to the position of *A* and *B*. *Figure modified from* Introduction to Genetic Analysis [63]

Complementation test and Deficiency Mapping

Deficiency chromosomes were used for complementation test and deficiency Mapping. The deficiency chromosomes are produced from chromosomal aberration or rearrangement in which a piece of the chromosome is excised and the remaining large pieces are reattached. TS paralytic behavior was analyzed at 36°C on the flies that carried the chromosome with the enhancer mutation in *trans* to a deficiency chromosome We expected that if the deficiency chromosome complemented the mutation, then the flies would not paralyze indicating that the mutated gene locus was not contained within from the region corresponding to the deficiency. Conversely, failure of complementation would indicate that the deficiency chromosome lacks the mutated gene (Figure 3.2**).**

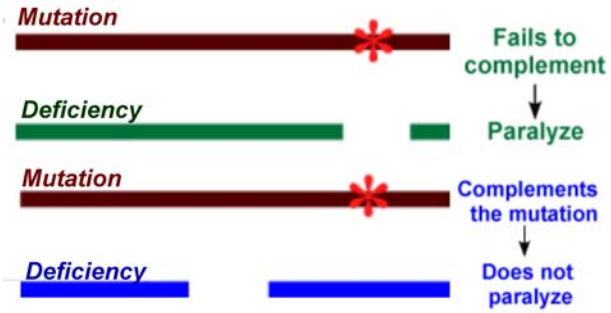

Figure 3.2: Complementation Test with deficiency chromosomes. The deficiency chromosomes (green and blue lines) are produced from chromosomal aberration or rearrangement in which a piece of the chromosome is excised and the remaining large pieces are reattached. If the mutation locus (marked with asterisk) fell within the region of deletion, deficiency chromosome would not complement the mutation, leading to TS paralytic behavior. Conversely, complementation would indicate that the mutation is not present in the region of deletion.

3.3 Results

3.3.1 Complementation Test with the Deficiency Chromosomes for Genes known to be involved in Synaptic Regulation

As a first step to map the location of a mutation, complementation tests were done to verify if the TS mutation fell within any gene already known to be involved in synaptic function. Some of the genes present in the second chromosome that are involved in the synaptic transmission are listed in Table 3.1. The males from the deficiency lines, *Df(2R)stan2* (deletion in *Rab3 synaptobrevin* gene), *Df(2L)FCK-20* (lacking Ca^{2+} *channel β subunit*), *Df(2R)27* (deficiency removing *synaptotagmin* gene) and *Df(2R)CB2* (deletion in *calmodulin* gene) were crossed to the virgin females heterozygous for *e(cac)2902* or *e(cac)3063* and homozygous for the cac^{TS2} mutation. The male progeny, which had cac^{TS2} on X-chromosome and enhancer mutation in *trans* to a deficiency

chromosome in the second chromosome, were tested for their TS behavior. All the deficiency chromosomes complemented the enhancer mutation, demonstrating that the mutation in the enhancer allele was not in the known genes. The result is summarized in Table 3.1.

Table 3.1: Complementation Test with Deficiency Chromosome for Known Genes

Candidate Gene	**Deficiency**	**Deleted Region (Cytological units)**	**Behavior at 36°C *wcac*^{TS2}; *2902* / *Df***	**Behavior at 36°C *wcac*^{TS2}; *3063* / *Df***
Ca^{2+} channel β subunit	Df (2L) FCK-20	32D1; 32F1	*cac*^{TS2}	*cac*^{TS2}
Calmodulin	Df (2R) CB21	48E; 49A	*cac*^{TS2}	*cac*^{TS2}
Rab3 and Synaptobrevin	Df (stan2)	46F1; 47B9	*cac*^{TS2}	*cac*^{TS2}
Synaptotagmin	In(2)syt^{D27}	23B1	*cac*^{TS2}	No progeny
	Df (N6)	23A6;23B1	No progeny	No progeny

3.3.2 Meiotic Mapping

For meiotic mapping, four visible markers, *Sternopleural (Sp), Scutoid (Sco), Lobed (L)* and *Pin* were used. The scheme for obtaining the recombinant flies is shown in Figure **3.3**. More than 400 flies were screened for each mutant line. Systematic analysis was not carried out, however crude recombinational mapping placed both the mutations *e(cac)2902* and *e(cac)3063* between *L* and *Pin* at an approximate region of 72-91 centi

Morgans (cM) on the basis of relative frequency with respect to the visible markers. The close proximity of mutation loci *e(cac)2902* and *e(cac)3063*, along with their similarity in the behavioral and synaptic phenotype suggested that they were two alleles of the same gene.

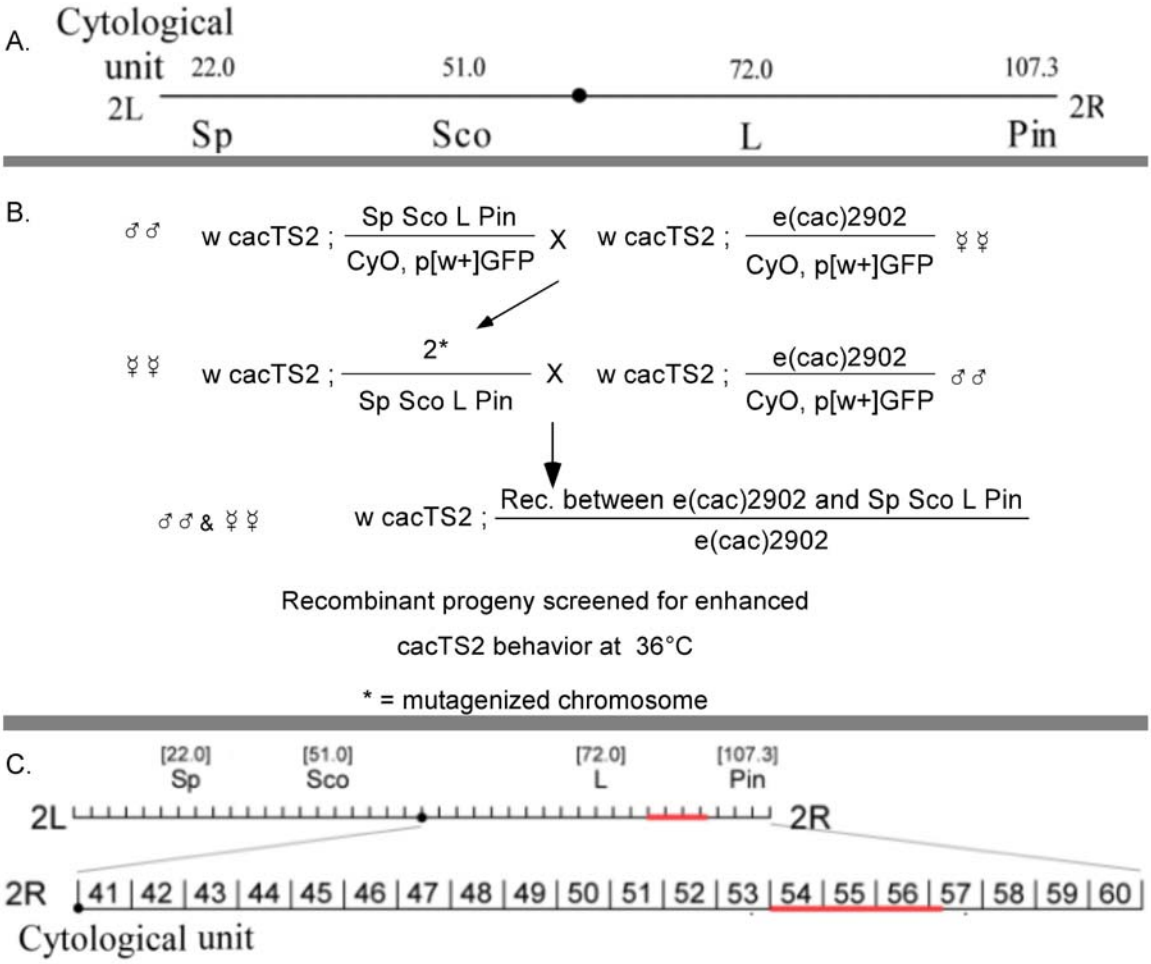

Figure 3.3: Meiotic Mapping. (A) The position of the visible markers in the second chromosome that were used for mapping. (B) The genetic scheme to produce recombinant flies.(C) Recombination mapping placed the mutation within 54A-57B cytological units (the region marked in red).

3.3.3 Deficiency Mapping

Meiotic mapping placed the locus of *e(cac)2902* and *e(cac)3063* on the right arm of the second chromosome between *L* and *Pin,* at 72-91 cM which corresponded to the 54A-57B cytological units [64]. To further define the region in which the locus resided, deficiency mapping was undertaken. Several deficiency lines were used to cover the region around the enhancer locus. We used the deficiency chromosomes from the Bloomington Stock Centre deficiency kit in which parts of the chromosome within the region 54A – 57A are deleted (Figure 3.4 A and B).

Two overlapping deficiencies, *Df(2R)BSC45* and *Df(2R)14H10Y-53* failed to complement both of the modifier mutations, *(cac)2902* and *e(cac)3063*. The *Df(2R)BSC45* lacked a region of ~200kbp from 54C8-54E7, while a region of ~150kbp between 54D1-54E7 was deleted in *Df(2R)14H10Y-53*. Comparing the two deficiencies, we concluded that the modifier locus fell within a region of ~150kbp between 54D1-54E7. To further narrow down the position of the locus, we carried out additional complementation tests using six lines with smaller deletions from the region 54D1-54E7. Two of the six deficiency lines, *Df (2R)Exel 7149* and *Df(2R)14F06W-10* failed to complement the enhancer mutations *e(cac)2902 and e(cac)3063* (Figure 3.4 C) and placed the mutation within a region of ~20kbp within 54D4-54D5.

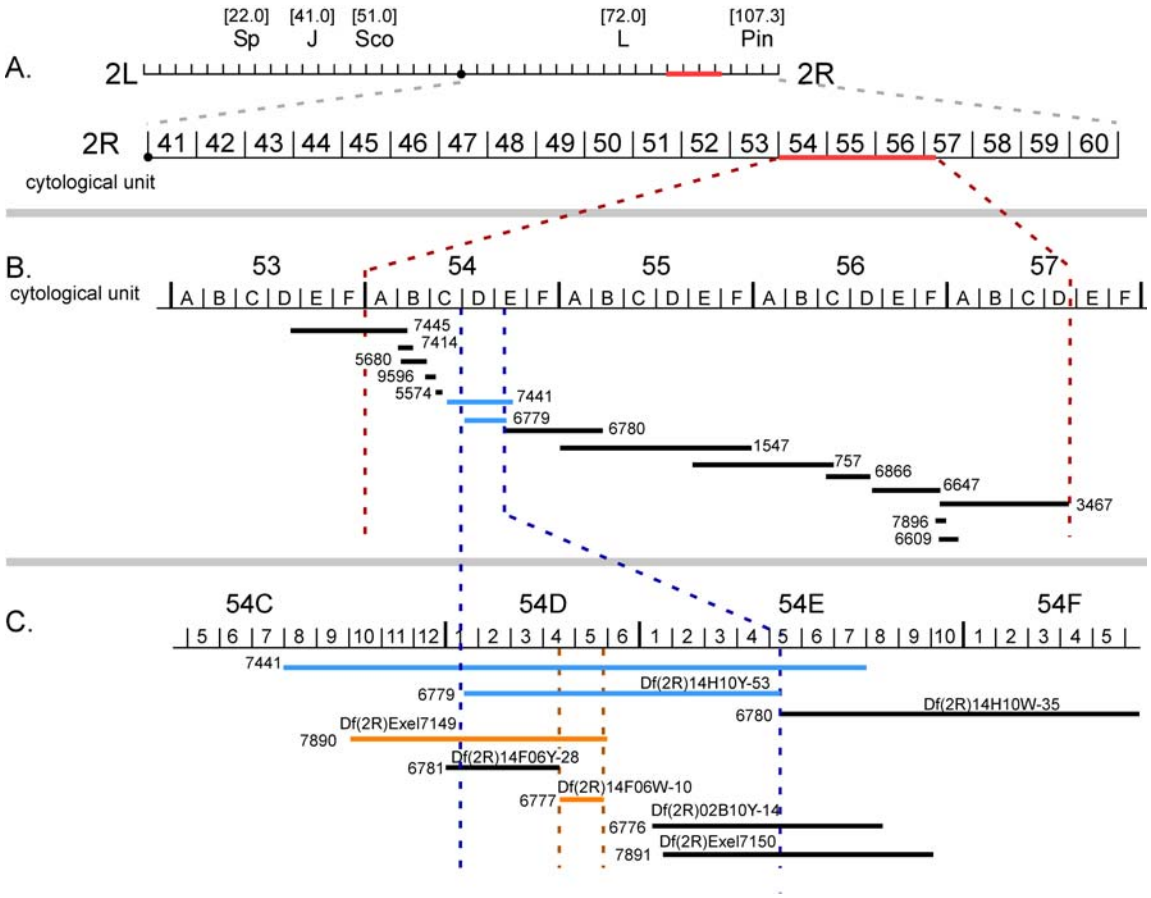

Figure 3.4: Deficiency Mapping for *e(cac)2902* and *e(cac)3063*. (A) Recombination mapping placed the mutation within cytological region 54A-57B. For narrowing down the region of mutation loci, deficiency chromosomes were used in which parts of the chromosome within the region 54A-57B was deleted. (B) The deletions in the deficiency chromosomes are shown as black or blue lines. The deficiencies represented by black lines complemented the mutations. The blue lines correspond to the deficiencies that failed to complement the enhancer mutations. The deficiency mapping suggested that the enhancer locus fell within a region of ~150kbp between 54D1-54E7 (C) Smaller deficiencies, indicated by blue, black or orange lines, were used to further reducing the region containing the enhancer locus. The orange lines correspond to the deficiencies that failed to complement the enhancer mutations and placed the mutation within a region of ~20kbp between 54D4-54D5.

The deficiency line *Df(2R)14F06W-10* was created by P-element deletion and thus the exact breakpoints for this deficiency had been mapped [65, 66]. A region of ~20 kbp

between the sequence co-ordinates 13553k - 13575k was deleted in this deficiency line. This deletion disrupted seven genes (Figure 3.5) as inferred from resources available in the Flybase website [67].

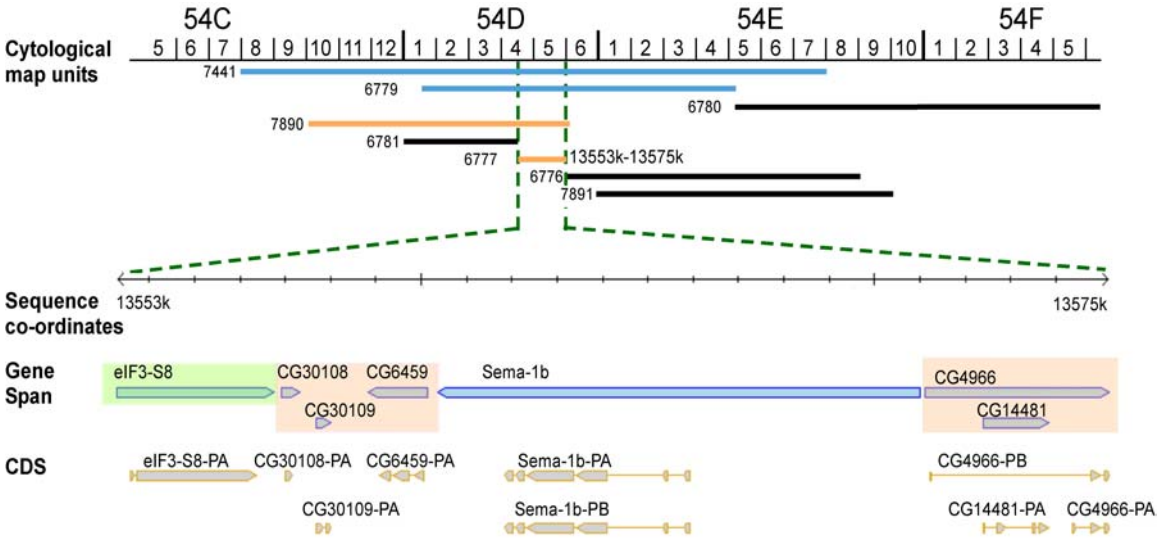

Figure 3.5: Candidate Genes present in the region containing the mutation loci for *e(cac)2902* and *e(cac)3063*. The mutation was mapped to the cytological map units 54D4-D5. This corresponded to the sequence co-ordinate 13553k-13575k. The spans of the seven genes that encompass this region are shown in this figure. The genes' coding sequences (CDS) are also shown.

3.4 Genes Present in the Region 54D1-54D4

Seven genes are present in the region containing the mutation locus for *e(cac)2902* and *e(cac)3063* (Figure **3.5**). These include *eIF3-S8, Sema1b, CG30108, CG30109, CG6459, CG4966* and *CG14481*. It may be noted that the mutations resulting in a TS paralytic phenotype typically map to coding sequence defined by the open reading frame (ORF) of the gene [58, 68, 69]. Here we have briefly reviewed the known

function(s) of the genes and the possibility of being the candidate gene causing TS paralytic phenotype.

eIF3-S8 (cytological map location 54D) is a translation initiation factor and is responsible for translational initiation. Any conditional mutation affecting translation would take a long time to exhibit its phenotype, whereas the TS mutants *e(cac)2902* and *e(cac)3063* paralyze very rapidly. Hence, we speculate that these mutations are least likely to be present in this gene.

The molecular function(s) of the genes *CG30108, CG30109, CG6459, CG4966* and *CG14481* are not known. *CG6459* is thought to be involved in the defense response to bacteria. The CG genes are predicted genes based on their DNA sequences. If the mutation lies in any of these genes, they will describe a novel function.

Semaphorin –1b or ***Sema-1b*** (cytological map location 54D4-54D5) is involved in intracellular signaling, receptor binding activity and cell surface receptor-linked signal transduction. It is a member of a large family of secreted and transmembrane proteins, some of which function as repellent signals during axon guidance. A role of *Sema-1b* in synaptic transmission would reveal a new function. The *Sema-1b* is a potential candidate whose function is related to neuronal function.

The modifier locus can be identified by sequence analysis of the candidate genes in the mutants. Sema-1b will be chosen initially for sequence analysis. But it is quite possible that the mutation does not reside in this gene and hence, other genes present in the region 54D4-54D5 will be sequenced. Mutation in any of the genes present in this region will reveal a novel function in synaptic transmission process. Though sequence

analysis is not a part of this thesis, it will be done in further characterization of the mutants.

Chapter 4

Discussion

We have reported the isolation and genetic characterization of two second chromosome enhancers of cac^{TS2} in this thesis. Both the mutations, *e(cac)2902* and *e(cac)3063* appear to be the alleles of the same gene. The behavioral and synaptic phenotypes, and genetic characterization of the enhancer mutation are described. The results reported here may further elucidate the in vivo interactions of *cac* encoded presynaptic calcium channels with other gene products in the neurotransmitter release process.

4.1 A screen for modifiers to identify genetic interactions with cac^{TS2}

Two main strategies for obtaining mutations are forward genetics and reverse genetics. Forward genetics starts with a phenotype of interest and seeks mutants of that phenotype for analysis. Reverse genetics starts with a gene sequence and seeks to find animals with the gene of interest mutated. Both approaches have the goal of relating genotype to phenotype, but forward genetics starts with the phenotype whereas reverse

genetics starts with the genotype. The aim of forward genetics is to identify mutations that produce a certain phenotype. Unbiased identification of genes is possible using forward genetics making it a very powerful tool. Forward genetic screens can be used to select for mutations in the entire genome. One limitation of this approach is that redundant genes or genes that do not play an important part under the set of conditions chosen for the mutant hunt may be missed.

In this project, a F_3 screen was undertaken. Even though F_3 screens are laborious and the reduced number of chromosomes examined is a major disadvantage, this approach allows screening for only recessive mutations in the germ line. Also, a population of flies can be screened compared to individual flies in F_1 screens. We screened for only recessive mutations, which often cause loss of function. It is also possible that some function may remain, but not at the level of the wild type allele. On the contrary, dominant mutations often give rise to products which interferes with the action of the normal protein or cause the gene product to gain a new activity. These altered functions of the mutated gene products can hinder the understanding of normal function of the gene product. Recessive mutations, therefore, are valuable tool for investigating gene functions.

In this project, two second chromosome enhancers of cac^{TS2}, *e(cac)2902* and *e(cac)3063*, were recovered. Both exhibited a striking enhancement of cac^{TS2} paralysis. The synaptic transmission defects in cac^{TS2} mutants were also enhanced in the presence of *e(cac)2902* or *e(cac)3063*. In a cac^{TS2} genetic background, the enhancers retained strong paralytic behavior and exhibited reduced synaptic current amplitudes compared to

wild type at restrictive temperature without cac^{TS2} in the background. These results indicated that the modifiers were capable of independent actions. Electrophysiological analysis showed that the current reduction was not activity dependent, suggesting the mutation may not affect vesicle trafficking. The paralytic and synaptic phenotypes of some of the well-characterized TS paralytic mutants is shown in Table 4.1. The immediate reduction of synaptic current was rather similar to the synaptic phenotype observed in TS mutants of ion channels such as cac^{TS2} [57].

Table 4.1: *Drosophila* TS Paralytic Mutants

TS Mutants	Gene product	Phenotype at restrictive temperature		Proposed Function
		Time for 50% paralysis	Synaptic phenotype	
shibire (shiTS1)	Dynamin GTPase	>1 min	Activity dependent decrease in evoked release	Endocytosis (Vesicle Trafficking)
comatose (comt)	NSF ATPase	1-2 mins	Activity dependent decrease in evoked release	Disassembly of SNARE
paralytic (para)	Na channel α_1 subunit	< 5 secs	-	Action potential
cacophony (cac)	Ca channel α_1 subunit	< 20secs	Evoked release reduced significantly	Presynaptic calcium influx
e(cac)2902	NOT KNOWN	< 15 seconds	Evoked release reduced significantly	NOT KNOWN

4.2 Genetic Mapping

In forward genetics, genetic mapping and molecular characterization of the corresponding genes usually follow recovery of mutations. A number of methods have been used for genetic mapping in *Drosophila*, including meiotic recombinational

mapping and deficiency mapping. Chromosomes carrying visible phenotypic markers, such as *Lobed*, in which the eyes are lobed or *Scutoid* where some or all the bristles in the posterior thorax are absent, are used in recombination mapping. The gene position is estimated on the basis of the recombination rate between markers and the locus of interest. Given the variation in recombination rates, recombinational mapping provides only a rough estimate of the gene position. An approximate region of 72-91 centiMorgans (cM) was estimated from recombinational mapping.

Deficiency mapping does not rely on recombination rates but rather on complementation analysis. It is a useful tool in mapping recessive mutations using a deficiency chromosome lacking a certain genomic region. Failure of complementation places the mutation within the genomic region removed in the deficiency. Several deficiency lines were used for this project and deficiency mapping placed the mutation in a region of ~20kbp between 54D4-54D5. This corresponded to the region we obtained from meiotic recombinational mapping, confirming that the region of mutation was predicted correctly. Seven genes are present in region 54D1-54D5 and further experiments are necessary to determine the gene in which the mutation resides.

4.3 Future directions

Identification of enhancers of cac^{TS2} raises the possibility of identifying molecules that interact with the calcium channel. Fine mapping has placed the enhancer locus in a small interval containing a limited number of candidate genes. The locus may be

identified by sequence analysis of the candidate genes in the mutants. Rescue of the mutant phenotype by expression of a transgenic candidate gene product will confirm that the candidate gene identified though sequence analysis is indeed the enhancer of the *cac*^{TS2} locus. Immunochemistry will be performed to study the subcellular localization of the candidate gene product, Western Blot will help determine its expression levels and protein-protein interactions may be examined by co-immunoprecipitation. The functional analysis, done in collaboration with other members, will complement the genetic and molecular studies. In brief, isolation of the modifiers of *cac*^{TS2} followed by genetic and molecular characterization will broaden our understanding of the *in vivo* role of specific gene products in synaptic transmission.

Chapter 5

Appendices

Appendix A:
Analysis of Synaptic Physiology in Transgenic Flies Expressing Tetanus Toxin

A.1 Introduction

Tetanus toxin is a powerful neurotoxic protein expressed by *Clostridium tetani*. The toxin is synthesized as a single polypeptide of 1315 amino acids. Preteolytic cleavage of the polypeptide yields two fragments: light chain (L_C) and heavy chain (H_C) joined by a disulphide bond (Figure A.1).

The tetanus toxin (TeTx) inhibits synaptic transmission and L_C mediates this effect. Internalization and translocation of the toxin into the cytosol of neurons is required to induce its toxic effect. Uptake of tetanus toxin in the neuronal cell occurs by vesicle-mediated endocytosis. After endocytosis, the toxin is exposed to the decreased pH inside the endocytosed vesicles. The low pH results in conformational change of the protein, which through a series of intermediate steps, results in the translocation of the light chain in the cytosol. The light chain cleaves a SNARE protein, synaptobrevin [70].

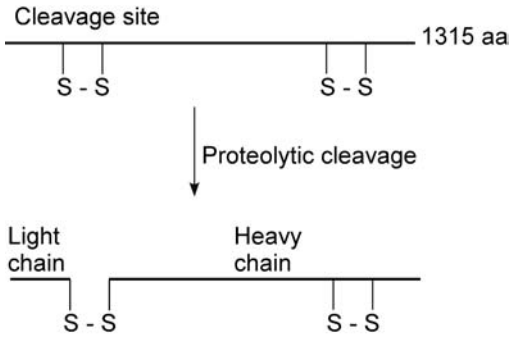

Figure A.1: Structure of tetanus toxin. The light chain (L_C) and a heavy chain (H_C) of tetanus toxin are formed by the proteolytic cleavage of a pre-protein. A disulphide linkage joins the L_C and the H_C.

Synaptobrevin is a SNARE protein that takes part in the fusion and exocytosis of the synaptic vesicles at the presynaptic terminal (as dicussed in chapter 1.3). As mentioned in chapter 1, synaptobrevin is present in the vesicle membrane and is termed as vesicle SNARE (v-SNARE) while the plasma membrane associated syntaxin and SNAP-25 are called target-SNAREs (t- SNARE) [20, 22] (Figure 1.6). During priming, the v- and t- SNAREs bind loosely to each other to form the "pre-fusion" intermediate referred to as a trans-SNARE complex. The fusion is complete when the fusion pore opens upon merging of the vesicular and presynaptic plasma membranes.

To further understand the role of SNARE proteins in synaptic fusion, the effect of TeTx transgene expression was studied in the nerve muscle junctions of third instar larva. Previous study by Sweeny *et al* [71] showed that presynaptic expression of the TeTx L_C eliminated synaptic transmission in the Drosophila embryo. We wanted to verify the effect of the toxin in the Drosophila nerve muscle junction (NMJ) of the third instar larvae.

A.2 Material and Methods

Fly Stocks

Fly stocks included OK6-Gal4; P{UAS-TNT}in which the TeTx trangene was expressed. *OK6-Gal4* drives expression in motor neurons beginning in the first instar larva until pupation. These flies were maintained at 25°C to increase the expression level of the transgene. Canton S (CS) was the wild type flies.

Dissection and Recording

Third instar larvae were dissected in slaine solution (in mM: 128 NaCl, 2 KCl, 4 $MgCl_2$, 1.8 $CaCl_2$, 36 sucrose, and 5 HEPES, pH, 7.0). Third instar larvae were cut open along the dorsal midline; digestive and other internal organs removed, the segmental nerves projecting from the ventral ganglion were cut close to the ganglion and larval brain and ventral ganglion were removed [72]. Two electrode voltage clamp recordings were carried out with temperature maintained at 20°C as described previously [73]. Glass microelectrodes were filled with 3M KCl. Synaptic currents were recorded from neuromuscular synapses of ventral longitudinal muscle6 in abdominal segment A2 or A3 at a holding potential of -60mV. Recordings were command potentials varied by more than 2mV were discarded.

A.3 Result

Two-electrode voltage clamp was used to record EPSCs from the nerve muscle junction (NMJ) of ventral longitudinal muscle 6 in abdominal segment A2 or A3. Recordings in flies expressing the trangene TeTx L_C were compared to those in wild-type (CS). Axons were stimulated at a low frequency of 1 Hz. Expression of the toxin in motor neurons elimininated synaptic transmission completely. The synaptic current amplitudes in WT and OK6-Gal4; UAS-TeTx were 227$\pm$ 37.27 nA (*n=8*) and 0nA (*n=3*) respectively (Figure A.2). Repeated stimulation also failed to produce any evoked current (data not shown).

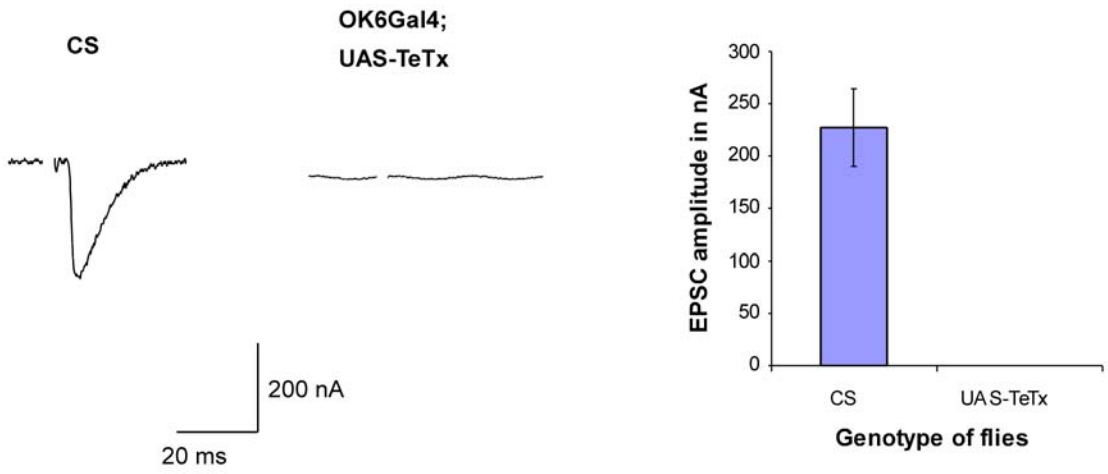

Figure A.2: Synaptic Physiology of OK6-Gla4; UAS-TNT (A) Representative Excitatory Postsynaptic Current (EPSC) recordings from neuromuscular synapses of muscle 6 of the abdominal segments A2 or A3 of wild type (WT) and OK6-Gla4; UAS-TNT at 20°C.. Stimulation artifacts were removed for clarity. OK6-Gla4; UAS-TNT flies were reared at 25°C (B) Mean EPSC amplitudes. SEM are represented by the error bars.

A.4 Discussion

Sweeney et al (1995) [71] had shown previously that presynaptic expression of TeTx blocked synaptic transmission completely in the embryo. In our experiment, we wanted to test if synaptic current was blocked in the larvae using a different driver to express the toxin. EPSCs were completely abolished in the larvae, verifying that the synaptic transmission was completely blocked. TeTx exerts its effect by cleaving synaptobrevin, a synaptic proetein. Thus, the properties of $TeTXL_C$ in Drosophila should make it a useful tool for analysis of synaptic transmission.

Appendix B:
Generation of transgenic fly lines carrying FLAG or tdTomato tagged calcium channel Beta subunit

B.1 Introduction

The β subunit of the calcium channel is an intracellular hydrophilic protein associated with the α_1 subunit. The β subunit plays an important role in trafficking and expression of functional calcium channels in the plasma membrane. It also plays an important role in biophysical properties of the channel; it hyperpolarizes the voltage dependence of activation of all VGCCs (smaller change in ΔV_m causes the channel to open). There are several phosphorylation sites in the β subunit that can be phosophorylated by protein kinases, which, in turn, can control the channel function. With all these functions, the β subunit appears to be more than a passive structural component of the calcium channels [41, 42]. Biochemical analysis (for example, protein - protein interaction or protein expression level) of the calcium channel β subunit, is constrained by the absence of a specific antibody against the protein. To overcome this challenge, calcium channel β subunit can be fused with a molecule that can be easily tracked. The transgenic flies carrying calcium channel β subunit fused with FLAG and tdTomato were thus produced.

FLAG is an octapeptide with amino acid sequence DYKDDDDK commonly used as a tag with proteins. Antibodies are available against FLAG, and this provides

advantages such as (a) purifying a FLAG-tagged protein, (b) studying the expression pattern by immunohistochemistry, (c) measuring the expression level by Western Blotting or (d) investigating the protein-protein interaction by co-immunoprecipitation. Generation of transgenic flies carrying FLAG-tagged calcium channel β subunit, therefore, would enable further study of the calcium channel function.

Fluorescent fusion proteins have emerged as a powerful tool to study gene expression and protein localization. They are used widely as donor/acceptor pairs for fluorescence resonance energy transfer (FRET) for investigating protein - protein interactions *in vivo.* The technique of FRET, when applied to optical microscopy, detects the approach between two molecules within several nanometers, a distance sufficiently close for molecular interactions to occur. In FRET, two different fluorescent molecules or fluorophores are genetically fused with the two proteins of interest. The red fluorescent protein tdTomato is a companion for the green fluorescent protein (GFP) in FRET.

B.2 Generation of DNA Construct carrying Calcium Channel β Subunit fused with FLAG or tdTomato

B.2.1 DNA construct of calcium channel β subunit – tdTomato transgene

To make the construct for calcium channel β subunit (from here onwards, referred only as β subunit) transgenes fused with tdTomato on the C terminus, a DNA clone of β subunit-EcoRI restriction site- eFGP fragement in pBluescript SK^+ (referred as clone A later) was used. This clone also contained a Hinc II site within the eGFP fragment. A blunt end cut was produced in this clone by digesting with Hinc II. Two oligonucleotides

were designed to create a BamHI restriction between β subunit and the eGFP. 1µl of both the oligos were mixed with 18µl 100mM NaCl. The mixture was denatured at 90ºC for three minutes and returned to room temperature until it cooled to ~25ºC.Then resulting annealed oligos were ligated into clone A using the HincII site. The ligation products were transformed into DH5α competent cells followed by plating on a 1.5% LB solid medium (10g tryptone, 5g yeast extract, 5g NaCl, 15g agar and 1ml 1N NaOH per liter) and culturing at 37ºC for 15 hours. Single colonies were isolated from the plated and cultured in 2XYT liquid medium (16g tryptone, 10g yeast extract and 5g NaCl per liter) at 37ºC with constant shaking for 15 hours. Plasmid DNA was extracted from the cultures by conventional methods. This plasmid DNA and transgenic construct, pBlurscipt SK^+ - cac- tdTomato that already existed in our lab was subjected to restriction digestion by SacII and BamHI. The restriction digestion of the plasmid DNA yielded a DNA fragment coding for β subunit and containing NotI and BamHI restriction sites on either end of the coding segment. On the other hand, tdTomato-pBluescriptII SK^+ was obtained from the transgenic construct, pBlursciptII SK^+ - cac- tdTomato. The DNA fragments, tdTomato-pBluescriptII SK^+ and DNA fragment coding for β subunit were extracted and purified by gel electrophoresis. The purified fragments were then ligated, transformed, cultured in liquid medium and plasmid DNA was extracted as described previously. Next, β subunit – tdTomato fragment was shuttled into the P-element based transfer vector, pUAST, using NotI and KpnI sites. This was followed by transformation into DH5α cells. Diagnostic digestion and sequencing were performed to verify the proper insertion and sequence of the transformed product. The pUAST- β subunit –tdTomato clone was cultured in 100 ml 2XYT liquid medium at 37ºC for 15 hours. DNA was prepared for

generation of transgenic flies using a midiprep kit (Qiagen). The DNA construct was quantified by performing a series of restriction digests and comparison with size standards on agarose gel.

B.2.2 DNA construct of calcium channel β subunit – FLAG transgene

FLAG tagged beta subunit of the calcium channel was previously cloned into the pBluescript II SK$^-$ vector. The construct was transformed into DH5α competent cells, and cultured on a 1.5% LB solid medium, cultured at 37ºC for 15 hours. Single colonies were isolated from the plate and cultured in 2XYT liquid medium. Plasmid DNA was extracted from the cultures by conventional methods. The beta subunt-FLAG fragment was then shuttled into the KpnI and NotI sites of the pUAST vector. The pUAST-beta subunit-FLAG clone was cultured in 100 ml 2XYT liquid medium for 15 hours., DNA was prepared for for generation of transgenic flies using a midiprep kit (Qiagen). DNA construct was verified for the correct clone by sequencing and quantified by a series of restriction digestion and comparing with size standards on agarose gel.

B.3 Generation of Transgenic Strains carrying tdTomato or FLAG-tagged β subunit of Calcium Channel

A few hundred w^{176} flies were reared in cages a few days prior to injection. Young embryos (younger than 30-minute-old) were collected from an egg laying plate for injection (4mm high, 90ml unsuphured molasses, 22g select agar, 250µl tegasept

stock and 556ml distilled H_2O) and transferred on a micro slide glass. All embryos were covered in oil (1:19 ratio of 27 Halocarbon oil to 700 Halocarbon oil, Sigma).

To prepare injection solution, plasmid DNA prepared using a Qiagen midiprep kit was diluted to ~0.8μg/μl and mixed with 10X 2μg/μl helper plasmid carrying a P-element transposase gene, 10X green food color (McCormick) and 10X injection buffer (50mM KCl, 1mM NaH_2PO_4 and 1mM Na_2HPO_4, pH 6.8). Prior to injection, needles were each filled with~1 μl injection solution.

Injection solution was injected into the posterior tip of each embryos contained in a micro slide glass that was placed on an upright microscope (Zeiss, Germany). After injection, cover glasses were placed on a fly food plate (100mm diameter and 13mm high) with up to eight cover glasses per plate. Plates were kept at room temperature. Two or three days after injection, F_0 larvae were transferred into vials with fresh fly food and kept at room temperature. Later, the F_0 adult flies were crossed individually according to the scheme in Figure B.1 Transgenic lines were selected and homozygous transgenic stocks established.

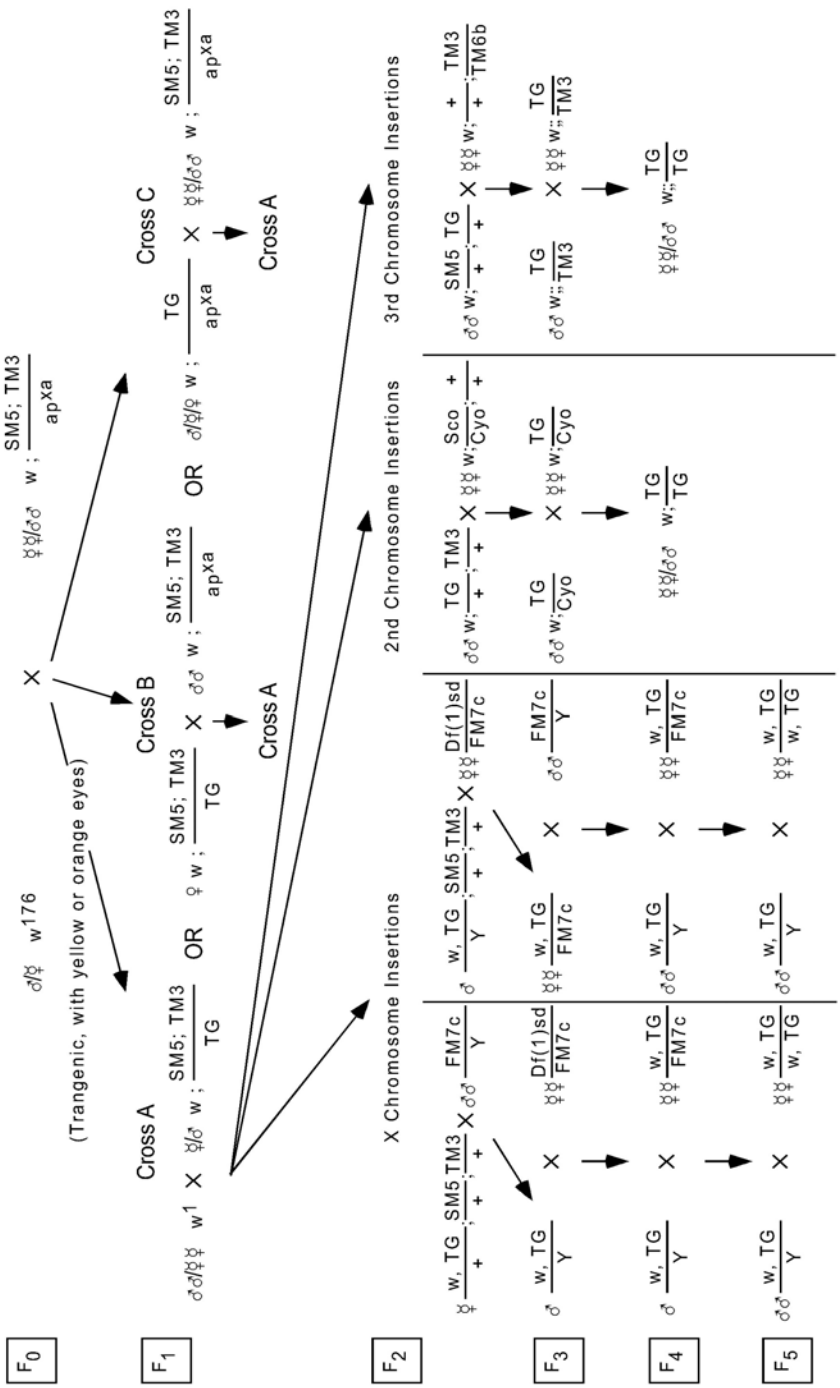

Figure B.1: Schematic illustrations crosses for developing homozygous stocks of transgenic lines

B.4 Verification of the Transgene Expression

B.4.1 β- FLAG

The expression level of the β -FLAG transgene was detected in the flies by Western Blot. The samples for Western Blot were prepared from fly heads. Fly heads were collected, homogenized in 1X SDS sample buffer and boiled for five minutes. The equivalent of two heads was loaded in each lane of a SDS-PAGE gel. The primary antibody was anti-FLAG used at a dilution of 1:500. Enhanced chemiluminescent reaction on the horse radish peroxidase (HRP) conjugated secondary antibody was used to detect the primary antibody. Tubulin, detected by the monoclonal anti-tubulin, was used to assess the concentration of the protein extract as an internal loading control. Out of 14 lines tested, the five lines expressed detectable levels of β FLAG (Figure B.2).

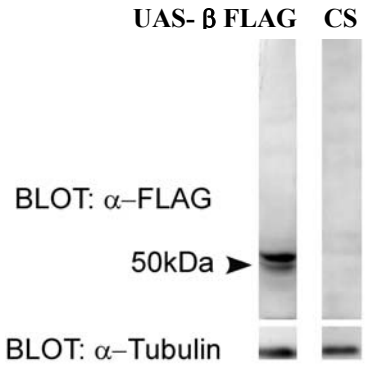

Figure B.2: Expression level of β-FLAG in the transgenic lines was detected by Western Blot. An anti-FLAG antibody was used to detect β FLAG (48.6 kDa). Only one line is shown in this figure as an example. The antibody also detected a nonspecific band in the transgenic line with molecular weight ~65KDa. Tubulin was used as a loading control.

B.4.2 Beta tdTomato

The expression level of the Beta-tdTomato transgene was detected by live imaging of the larval neuromuscular junction. Third-instar larvae were dissected in saline solution (in mM: 128 NaCl, 2 KCl, 4 MgCl2, 1.8 CaCl2, 36 sucrose, and 5 HEPES, pH, 7.0), and all nerves projecting from the ventral ganglion were cut to prevent muscle contraction. Epifluorescence images were obtained using a Nikon (Tokyo, Japan) Eclipse E600FN microscope with a Fluor 60X 1.0 numerical aperture water-immersion objective (Nikon). Images were captured with a CCD camera (ORCA-ER; Hamamatsu Photonics, Hamamatsu, Japan) and acquired and processed using the Metavue imaging software package (Universal Imaging Corporation). In this study, all images of larval neuromuscular synapses were obtained from ventral longitudinal muscles 6 and 7 within abdominal segment A2 or A3. An example of the image is shown in Figure B.3.

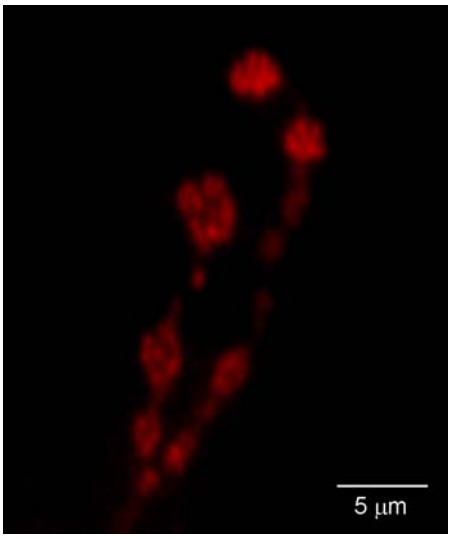

Figure B.3: Live imaging of β-tdTomato at larval neuromuscular synapses. Images were acquired with a Nikon (Tokyo, Japan) Eclipse E600FN microscope equipped with a Fluor 60X 1.0 numerical aperture water-immersion objective (Nikon) and the following filter set: excitation filter, 555/25; dichroic mirror, 565DCLP; and emission filter, D620/60 (Chroma, Brattleboro, VT). Image capture was carried out using a CCD camera (ORCA-ER; Hamamatsu Photonics, Hamamatsu, Japan) controlled by MetaVue software (Universal Imaging, Ypsilanti, MI).

Bibliography

1. Rosenmund, C., Rettigy, J. and Brosez, N., *Molecular mechanisms of active zone function.* Current Opinion in Neurobiology, 2003. **13**: p. 509-519.
2. Zhai, R.G.a.B., Hugo J., *The Architecture of the Active Zone in the Presynaptic Nerve Terminal.* Physiology, 2004. **19**: p. 262-270.
3. Kittel, R.J., et al., *Active zone assembly and synaptic release.* Biochemical Society Transactions, 2006. **34**(Pt 5): p. 939-941.
4. Kittel, R.J., et al., *Bruchpilot Promotes Active Zone Assembly, Ca2+ Channel Clustering, and Vesicle Release.* Science, 2006. **312**(5776): p. 1051-1054.
5. Juranek, J., et al., *Differential expression of active zone proteins in neuromuscular junctions suggests functional diversification.* European Journal of Neuroscience, 2006. **24**(11): p. 3043-3052.
6. Prokop, A. and I.A. Meinertzhagen, *Development and structure of synaptic contacts in Drosophila.* Seminars in Cell & Developmental Biology, 2006. **17**(1): p. 20-30.
7. Murthy, V.N. and C.F. Stevens, *Reversal of synaptic vesicle docking at central synapses.* Nat Neurosci, 1999. **2**(6): p. 503-507.
8. Sudhof, T.C., *THE SYNAPTIC VESICLE CYCLE*. 2004. p. 509-547.
9. Fernandez-Alfonso, T. and T.A. Ryan, *The kinetics of synaptic vesicle pool depletion at CNS synaptic terminals.* Neuron, 2004. **41**: p. 943-953.
10. Fernandez-Alfonso, T. and T.A. Ryan, *The efficiency of the synaptic vesicle cycle at central nervous system synapses.* Trends in Cell Biology, 2006. **16**(8): p. 413-420.
11. Matthews, G., *Minireview Cycling the Synapse:Scenic versus Direct Routes for Vesicles.* Neuron, 2004. **44**: p. 223–226.
12. Aravanis, A.M., Pyle, J. L. and Tsien,R.W, *Single synaptic vesicles fusing transiently and successively without loss of identity.* Nature, 2003. **523**: p. 643-647.
13. Gandhi SP, S.C., *Three modes of synaptic vesicular recycling revealed by single-vesicle imaging.* Nature, 2002. **423**: p. 607-613.
14. Granseth, B., et al., *Clathrin-mediated endocytosis the physiological mechanism of vesicle retrieval at hippocampal synapses*. 2007. p. jphysiol.2007.139022.
15. Rizzoli, S.O. and R. Jahn, *Kiss-and-run, Collapse and â€˜Readily Retrievableâ€™ Vesicles*. 2007. p. 1137-1144.
16. Rizzoli, S.O. and W.J. Betz, *Synaptic vesicle pools.* Nat Rev Neurosci, 2005. **6**(1): p. 57-69.
17. Rizzoli, S.O. and W.J. Betz, *The Structural Organization of the Readily Releasable Pool of Synaptic Vesicles.* Science, 2004. **303**(5666): p. 2037-2039.
18. Weber, T., et al., *SNAREpins: Minimal Machinery for Membrane Fusion.* Cell, 1998. **92**(6): p. 759-772.
19. Clary, D., Griff, I. C., and Rothman, J.E., *SNAPs, A Family of NSF Attachment Proteins Involved in Intracellular Membrane Fusion in Animals and Yeast.* Cell, 1990. **61**: p. 709-721.

20. Söllner, T., Whiteheart, S.W., Brunner, M., Erjument-Bromage, H., Geromanos, S., Tempst, P., Rothman, J., *SNAP receptors implicated in vesicle targeting and fusion.* Nature, 1993. **362**: p. 318-324.
21. Wilson, D.W., Wilcox, C. A., Flynn, G.C., Chen, E., Kuang, W., Henzel, W.J. Block, M.R., Ulrich, A. and Rothman, J.E., *A fusion protein required for vesicle-mediated transport in mammalian cells and yeast.* Nature, 1989. **339**: p. 355-359.
22. Jahn, R. and R.H. Scheller, *SNAREs [mdash] engines for membrane fusion.* Nat Rev Mol Cell Biol, 2006. **7**(9): p. 631-643.
23. Brunger, A.T., *Structure and functionof SNARE and SNARE-interacting proteins.* Quarterly Reviews of Biophysics, 2006. **38**(1): p. 1-47.
24. Barnard, R.J.O., A. Morgan, and R.D. Burgoyne, *Stimulation of NSF ATPase Activity by α-SNAP Is Required for SNARE Complex Disassembly and Exocytosis.* The Journal of Cell Biology. **139**(4): p. 875–883.
25. Salaun, C., et al., *Plasma membrane targeting of exocytic SNARE proteins.* Biochimica et Biophysica Acta (BBA) - Molecular Cell Research, 2004. **1693**(2): p. 81-89.
26. Toonen, R.F.G. and M. Verhage, *Vesicle trafficking: pleasure and pain from SM genes.* Trends in Cell Biology, 2003. **13**(4): p. 177-186.
27. Toonen, R.F.G., *Role of Munc18-1 in synaptic vesicle and large dense-core vesicle secretion.* Biochemical Society Transactions, 2003. **31**(Pt 4): p. 848-850.
28. Becherer, U. and J. Rettig, *Vesicle pools, docking, priming, and release.* Cell and Tissue Research, 2006. **326**(2): p. 393-407.
29. Jahn, R., T. Lang, and T.C. Sudhof, *Membrane Fusion.* Cell, 2003. **112**(4): p. 519-533.
30. Jahn, R. and T.C. Sudhof, *MEMBRANE FUSION AND EXOCYTOSIS.* Annual Review of Biochemistry, 1999. **68**(1): p. 863-911.
31. Zamponi, G.W., *Voltage-Gated Calcium Channels*. 2005: Springer. 377 pages.
32. Evans, R.M. and G.W. Zamponi, *Presynaptic Ca2+ channels - integration centers for neuronal signaling pathways.* Trends in Neurosciences, 2006. **29**(11): p. 617-624.
33. Catterall, W.A., *Structure and Regulation of Voltage-Gated Ca^{2+} Channels.* Annu. Rev. Cell Dev. Biol, 2000. **16**: p. 521–55.
34. Van Petegem, F. and D.L. Minor, *The structural biology of voltage-gated calcium channel function and regulation.* Biochemical Society Transactions, 2006. **34**(Pt 5): p. 887-893.
35. Caterall, W.A., et al., *International Union of Pharmacology. XLVIII. Nomenclature and Structure-Function Relationships of Voltage-Gated Calcium Channels.* Pharmacological Reviews, 2005. **57**: p. 411–425.
36. Xie, C., X.-g. Zhen, and J. Yang, *Localization of the Activation Gate of a Voltage-gated Ca^{2+} Channel.* The Journal of General Physiology, 2005. **126**(3): p. 205-212.
37. Seagar, M., et al., *Interactions between proteins implicated in exocytosis and voltage-gated calcium channels.* Philosophical Transactions of the Royal Society B: Biological Sciences, 1999. **354**(1381): p. 289-297.

38. Erickson, M.G., et al., *Preassociation of Calmodulin with Voltage-Gated Ca2+ Channels Revealed by FRET in Single Living Cells.* Neuron, 2001. **31**(6): p. 973-985.
39. Hidalgo, P., et al., *The α_1-β Subunit Interaction That Modulates Calcium Channel Activity Is Reversible and Requires a Competent α-Interaction Domain*.* The Journal of Biological Chemistry, 2006. **281**(34): p. 24104–24110.
40. Richards, M.W., Butcher, A.J. and Annette C. Dolphin, *Ca2C channel b-subunits: structural insights AID our understanding.* TRENDS in Pharmacological Sciences 2004. **25**(12): p. 626-632.
41. Dolphin, A.C., *β subunits of voltage-gated calcium channels.* Journal of Bioenergetics and Biomembranes, 2003. **35**(6): p. 599-620.
42. Brice, N.L., et al., *Importance of the Different p Subunits in the Membrane Expression of the a l A and a2 Calcium Channel Subunits: Studies Using a Depolarization-sensitive a1 A Antibody.* European Journal of Neuroscience, 1997. **9**: p. 749-759.
43. Davies, A., et al., *Functional biology of the [alpha]2[delta] subunits of voltage-gated calcium channels.* Trends in Pharmacological Sciences, 2007. **28**(5): p. 220-228.
44. Chaudhuri, D., J.B. Issa, and D.T. Yue, *Elementary Mechanisms Producing Facilitation of Cav2.1 (P/Q-type) Channels.* The Journal of General Physiology, 2007. **129**(5): p. 385-401.
45. Yoshihara, M. and J.T. Littleton, *Synaptotagmin I Functions as a Calcium Sensor to Synchronize Neurotransmitter Release.* Neuron, 2002. **36**: p. 897–908.
46. Kawasaki, F., R. Felling, and R.W. Ordway, *A Temperature-Sensitive Paralytic Mutant Defines a Primary Synaptic Calcium Channel in Drosophila*. 2000. p. 4885-4889.
47. Quinn, W.G. and J.L. Gould, *Nerves and genes.* Nature, 1979. **278**: p. 19-24.
48. Venken, K.J.T. and H.J. Bellen, *Emerging Technologies for Gene Manipulation In Drosophila melanogaster* Nature Reviwes, Genetics, 2004. **6**(2005): p. 167.
49. Celotto, A.M. and M.J. Palladino, *Fly Models of Neurodegeneration.* Molecular Intervention, 2005. **5**(5): p. 292-303.
50. Ikeda, K., S. Ozawa, and S. Hagiwara, *Synaptic transmission reversibly conditioned by single-gene mutation in Drosophila melanogaster.* Nature, 1976. **259**: p. 489-491.
51. Vijayakrishnan, N., and Broadie, K., *Temperature-sensitive paralytic mutants: insights into the synaptic vesicle cycle.* Biochem. Soc. Trans., 2006. **34**: p. 81–87.
52. Benzer, O.S.a.S., *Neurophysiological defects in temperature-sensitive paralytic mutants of Drosophila melanogaster.* Proc Natl Acad Sci U S A, 1976. **73**(9): p. 3253–3257.
53. Suzuki, D.T., T. Grigliatti, and R. Williamson, *Temperature-Sensitive Mutations in Drosophila melanogaster, VII. A Mutation (parats) Causing Reversible Adult Paralysis.* Proc. Nat. Acad. Sci. USA, 1971. **68**(5): p. 890-893.
54. Kawasaki, F., A.M. Mattiuz, and R.W. Ordway, *Synaptic Physiology and Ultrastructure in comatose Mutants Define an In Vivo Role for NSF in Neurotransmitter Release*. 1998. p. 10241-10249.

55. Pallanck, L., R.W. Ordway, and B. Ganetzky, *A Drosophila NSF mutant.* Nature, 1995. **376**(6535): p. 25-25.
56. Tolar, L.A. and L. Pallanck, *NSF Function in Neurotransmitter Release Involves Rearrangement of the SNARE Complex Downstream of Synaptic Vesicle Docking*. 1998. p. 10250-10256.
57. Dellinger, B., R. Felling, and R.W. Ordway, *Genetic Modifiers of the Drosophila NSF Mutant, comatose, Include a Temperature-Sensitive Paralytic Allele of the Calcium Channel {alpha}1-Subunit Gene, cacophony*. 2000. p. 203-211.
58. Kawasaki, F., S.C. Collins, and R.W. Ordway, *Synaptic Calcium-Channel Function in Drosophila: Analysis and Transformation Rescue of Temperature-Sensitive Paralytic and Lethal Mutations of Cacophony*. 2002. p. 5856-5864.
59. Kulkarni, S.J. and J.C. Hall, *Behavioral and Cytogenetic Analysis of the cacophony Courtship Song Mutant and Interacting Genetic Variants in Drosophila melanogaster.* Genetics, 1987. **115**(3): p. 461-475.
60. Kulkarni, S.J., A.F. Steinlauf, and J.C. Hall, *The dissonance Mutant of Courtship Song in Drosophila melanogaster: Isolation, Behavior and Cytogenetics.* Genetics, 1988. **118**(2): p. 267-285.
61. Smith, L.A., et al., *Courtship and Visual Defects of cacophony Mutants Reveal Functional Complexity of a Calcium-Channel {alpha}1 Subunit in Drosophila*. 1998. p. 1407-1426.
62. Brooks, I.M., et al., *Genetic Analysis of a Synaptic Calcium Channel in Drosophila: Intragenic Modifiers of a Temperature-Sensitive Paralytic Mutant of cacophony*. 2003. p. 163-171.
63. Griffiths, A.J.F.M., Jeffrey H.; Suzuki, David T.; Lewontin, Richard C.; Gelbart, William M., *Introduction to Genetic Analysis.* . 7th ed. 1999, New York: W. H. Freeman & Co.
64. http://flybase.bio.indiana.edu/static_pages/docs/cytotable3.html. *Map Conversion Table*. [cited.
65. Huet, F., et al., *From the Cover: A deletion-generator compound element allows deletion saturation analysis for genomewide phenotypic annotation.* Proceedings of the National Academy of Sciences, 2002. **99**(15): p. 9948-9953.
66. Mohr, S.E. and W.M. Gelbart, *Using the P{wHy} Hybrid Transposable Element to Disrupt Genes in Region 54D-55B in Drosophila melanogaster.* Genetics, 2002. **162**(1): p. 165-176.
67. http://flybase.bio.indiana.edu/cgi-bin/gbrowse/dmel/. 2008 [cited R5.5; Jan 2008.
68. Rao, S.S., Stewart, B.A., Rivlin, P.K., Vilinsky, I,. Watson, B.O., Lang, C., Boulianne, G., Salpeter, M.M., and Deitcher, D., L., *Two distinct effects on neurotransmission in a temperature-sensitive SNAP-25 mutant.* EMBO J., 2001. **20**(23): p. 6761–6771.
69. Rikhy, R., M. Ramaswami, and K.S. Krishnan, *A Temperature-Sensitive Allele of Drosophila sesB Reveals Acute Functions for the Mitochondrial Adenine Nucleotide Translocase in Synaptic Transmission and Dynamin Regulation.* Genetics, 2003. **165**(3): p. 1243-1253.
70. Linka, E., Edelmanna, L., Choua, J. H., Binzc, T., Yamasakic, S., Eiseld, U., Baumerte, M., Südhofe, T.C., Niemannc, H., Jahn, R. , *Tetanus toxin action:*

Inhibition of neurotransmitter release linked to synaptobrevin proteolysis. Biochemical and Biophysical Research Communications 1992. **189**(2): p. 1017-1023.

71. Sweeney, S.T., Broadie, K. , Keanea, J., Niemannc, H. and O'Kanea, C.J., *Targeted expression of tetanus toxin light chain in Drosophila specifically eliminates synaptic transmission and causes behavioral defects.* Neuron, 1995. **14**(2): p. 341-351.
72. Jan, L.Y. and Y.N. Jan, *Properties of the larval neuromuscular junction in Drosophila melanogaster.* The Journal of Physiology Online, 1976. **262**(1): p. 189-214.
73. Kawasaki, F., A.M. Mattiuz, and R.W. Ordway, *Synaptic Physiology and Ultrastructure in comatose Mutants Define an In Vivo Role for NSF in Neurotransmitter Release.* Journal of Neuroscience, 1998. **18**(24): p. 10241-10249.

VITA

SHAONA ACHARJEE
sua130@psu.edu

208 Mueller lab
Pennsylvania State University,
University Park, PA 16802
Phone 814 865 3076

411 Waupelani Drive,
Apertment # A-301
State College, PA-16801
Phone 814 441 1534

EDUCATION

Ph.D. in Biology, *Pennsylvania State University* *GPA: 3.8/4.0* PA, USA
Major: Biology (Molecular neuroscience) May 2008

M.S. in Biophysics and Molecular Biology, University of Calcutta Kolkata, India
July 2003

B.S. with Honors in Physiology, University of Calcutta, India Kolkata, India
July 2001

PUBLICATION

Abstracts Published:

- *Shaona Acharjee, Andrew Lutas and Fumiko Kawasaki*. A genetic screen for second chromosome modifiers of a temperature-sensitive presynaptic calcium channel mutant of *Drosophila*. Neurobiology of *Drosophila* Meeting at Cold Spring Harbor Laboratory, New York, October 2007
- *S. Acharjee, S.Q.J. Liu.* Action potential duration regulates targeting of GLUR2- containing AMPA receptors to the parallel fibre-stellate cell synapse.Annual Meeting of Society for Neuroscience, San Diego, Oct. 2004

AWARDS/ FELLOWSHIPS

- Braddock Fellowship from Eberly College of Science, Penn State University 2008 & 2003-2004
- Summer Project Fellowship by the TIFR, Mumbai, India 2002
- *Summer Project Fellowship* by Jawaharlal Nehru Center for Advanced Scientific Research, Bangalore (India). 2001

TEACHING AND SUPERVISORY EXPERIENCE

- **Teaching Assistant**, Dept. of Biology, Penn State University 2008, 2004-05
- **Teaching Assistant Co-ordinator,** Dept. of Biology, Penn State University 2007